

Soil Erosion Assessment Using Remotely Sensed Data and Ancillary Data in the Desert Of Tabernas, southeast Spain

Yared Jillo Gobena
, 2003

Soil Erosion Assessment Using Remotely Sensed Data and Ancillary Data in the Desert Of Tabernas, southeast Spain

by

Yared Jillo Gobena

Thesis submitted to the International Institute for Geo-information Science and Earth Observation in partial fulfilment of the requirements for the degree in Master of Science in *Geo-information Science and Earth Observation, Environmental System Analysis and Monitoring specialization*.

Degree Assessment Board

Thesis advisor	Dr. Tsehaie Woldai prof. Dr. Freek van der Meer
Thesis examiners	prof. Dr. Freek van der Meer (Chairman) Dr. K.Hein UU (External Examiner) Dr. Dr. D.P. Shrestha (Member) Dr. P.M. van Dijk (PD) (Observer)



INTERNATIONAL INSTITUTE FOR GEO-INFORMATION SCIENCE AND EARTH OBSERVATION
ENSCHDE, THE NETHERLANDS

Disclaimer

This document describes work undertaken as part of a programme of study at the International Institute for Geo-information Science and Earth Observation (ITC). All views and opinions expressed therein remain the sole responsibility of the author, and do not necessarily represent those of the institute.

Contents

List of Figures	iii
List of Tables	v
Acknowledgements	vii
Abstract	ix
1 INTRODUCTION	1
1.1 ENVIRONMENTAL PROBLEMS IN THE STUDY AREA	3
1.2 PREVIOUS ACTIVITIES	4
1.3 RESEARCH OBJECTIVES	5
1.4 IMPORTANCE OF THE RESEARCH	5
1.5 METHODOLOGY	5
1.6 RESEARCH MOTIVATIONS	6
1.7 HYPOTHESIS	7
1.8 RESEARCH OUTLINE	7
2 DESCRIPTION OF THE STUDY AREA	9
2.1 LOCATIONS AND ACCESS	9
2.2 CLIMATE	10
2.3 GEOMORPHOLOGY	11
2.4 SOILS	13
2.5 LAND COVER	14
2.5.1 CHANGES IN LAND COVER	14
2.6 LAND USE	15
2.6.1 CHANGES IN LAND USE	15
2.7 GEOLOGIC PROCESSES AND LAND DEGRADATION	16
2.8 INFRASTRUCTURE DEVELOPMENT (ROAD)	16
3 GEOLOGY AND STRUCTURE	17
3.1 METAMORPHIC ROCKS OF THE BETIC ZONE	18
3.2 NEVADO-FILABRIDE COMPLEX	18
3.3 ALPUJARRIDE COMPLEX	19
3.4 MALAGUIDE COMPLEX	20
3.5 SEDIMENTARY SUCCESSION	20
3.6 QUATERNARY DEPOSITS	21

3.7	GEOLOGY AND ENVIRONMENT	22
4	MATERIAL, RESEARCH METHODS AND TECHNIQUES	23
4.1	INTRODUCTION	23
4.2	MATERIALS	23
4.3	METHODOLOGY	24
4.4	DATA ANALYSIS, IMAGE PROCESSING AND INTERPRETATION OF REMOTE SENS- ING AND GIS DATA	24
4.4.1	DATA ANALYSIS	24
4.4.2	IMAGE DATA HANDLING	24
4.4.3	SPATIAL DATA ANALYSIS	25
4.4.4	COLOUR COMPOSITE	26
4.4.5	NORMALIZED DIFFERENCE VEGETATION INDEX (NDVI)	26
4.5	CONCLUSIONS	28
5	SOIL EROSION (SOIL LOSS) ASSESSMENT	29
5.1	INTRODUCTION	29
5.1.1	SHEET EROSION	29
5.1.2	GULLY EROSION	30
5.2	CLASSIFICATION OF PHYSIOGRAPHIC ZONES FOR SEDIMENT GENERATION AND DEPOSITION	31
5.3	PREDICTION OF SOIL EROSION BY WATER USING RUSLE	32
5.3.1	RAINFALL-RUNOFF EROSIVITY FACTOR (R)	34
5.3.2	SOIL ERODIBILITY FACTOR (K)	36
5.3.3	SLOPE LENGTH AND SLOPE STEEPNESS FACTORS (LS)	40
5.3.4	COVER-MANAGEMENT FACTOR (C)	43
5.3.5	CONSERVATION PRACTICE FACTOR (P)	44
5.3.6	SOIL LOSS (A)	44
5.4	CONCLUSIONS	47
6	RESULTS ANALYSIS AND DISCUSSION	49
6.1	INTRODUCTION	49
6.2	RAINFALL-RUNOFF EROSIVITY FACTOR (K)	49
6.3	SOIL ERODIBILITY FACTOR (K)	51
6.4	SLOPE LENGTH AND SLOPE STEEPNESS FACTOR (LS)	52
6.5	COVER-MANAGEMENT FACTOR (C)	52
6.6	SENSITIVITY ANALYSIS	52
7	CONCLUSIONS AND RECOMMENDATIONS	57
7.1	CONCLUSIONS	57
7.2	RECOMMENDATIONS	58
	References	59
8	APPENDICES	63

List of Figures

1.1	Operational Flow Chart.	6
2.1	Location map of the Tabernas Basin (the study area).	9
2.2	Monthly Precipitation, potential evapotranspiration and temperature in Tabernas area.	11
2.3	Badlands geomorphology of the Tabernas area [20].	12
3.1	Geological Setting of the Betic Cordilleras [63].	18
3.2	Graphite mica schist (light-dark) and Tahal schist (light-brown) (GRMEG, 2002).	19
3.3	Turbiditic sandstone and marl overlain unconformably by conglomerate (Chozas Formation).	20
3.4	Geological map of study area (GRMEG, 2002).	21
4.1	False colour composites (vegetation: Reddish; bareland: DimGray and Grey and water: Bluish).	26
4.2	Map of NDVI.	27
4.3	Map of NDVI Classified.	28
5.1	Uplifted and faulted Miocene marls (Chozas Formation) are being eroded by surface processes, leading to the formation of gully and valleys (Mitchell, 1995).	30
5.2	Map of DEM of study area.	31
5.3	Map of physiographic zones.	32
5.4	General Flow Chart of RUSLE.	33
5.5	Textural classes for soil erodibility prediction.	37
5.6	Map of categories of soil vulnerability to erosion and deposition areas.	38
5.7	Estimated soil erodibility factor (K) by the equation of Wischmeier soil-erodibility nomograph, and K in [ton/ha per MJ/ha*mm/yr].	39
5.8	Estimated soil erodibility factor (K) by mean geometric particle size (world soil data set) method and K in [ton/ha per MJ/ha*mm/hr].	40
5.9	Map of erosion risk categories.	41
5.10	Map of LS factor with value ranges from 0.128-12.248.	43
5.11	Table of land cover classes.	44
5.12	Table of annual soil loss (A) for soil with organic matter and dots indicate that the continuation of values for each grid cells.	45
5.13	Table of annual soil loss (A) for soil without organic matter and dots indicate that the continuation of values for each grid cells.	46
5.14	Map of annual soil loss (A1) for soil sample with organic matter and values vary for each grid cells ranging from 0.15-14.55 ton/grid cells.	48

5.15	Map of annual soil loss (A2) for soil sample without organic matter and values vary for each grid cells ranging from 0.41-38.81 ton/grid cells.	48
6.1	Table of typical annual erosivity range classification in different unit systems [15] . .	50
6.2	Graph of monthly rainfall amounts and associated sum of square of monthly rainfall per annual rainfall	51
6.3	Graph of soil erodibility as a function of mean geometric particle diameter (Dg) in S.I.units or (ton/ha per MJ/ha*mm/hr)	52
6.4	Graph of Slope length factor (L) and Slope steepness factor (S) vs Soil loss (A) . . .	54
6.5	Graphs of Slope factors (LS) and Slope % (SLOPEPCT) vs soil loss (A)	55
6.6	Graph of Rainfall erosivity factor(R) vs Soil loss (A)	55
6.7	Graph of Soil erodibility factor (K) vs soil loss (A)	56
6.8	Graph of Cover management factor (C) vs Soil loss (A)	56
8.1	Map of degraded and bad land geomorphology in Tabernas area	63
8.2	Table of Rainfall and Temperature data for Almeria area from Spanish Meteorological Office (1968-1990).	64
8.3	Example of equation of mean geometric particle diameter(word data set)	65
8.4	Table of soil texture data (Tilahun, 2002)	65
8.5	Table of coordinate system and sample number for soil texture data (Tilahun, 2002) .	66
8.6	Table of ILWIS 3.0 RUSLE Topographic Factor (LS) interface for soil loss estimated per grid cells that continued from chapter 5 and; K1 and A1 indicates values for soil with organic matter while K2 and A2 indicates values for soil without organic matter . .	66
8.7	Table of ILWIS 3.0 RUSLE Topographic Factor (LS) interface for soil loss estimated per grid cells continued.	67
8.8	Table of ILWIS 3.0 RUSLE Topographic Factor (LS) interface for soil loss estimated per grid cells continued.	67
8.9	Table of ILWIS 3.0 RUSLE Topographic Factor (LS) interface for soil loss estimated per grid cells continued.	68
8.10	Table of ILWIS 3.0 RUSLE Topographic Factor (LS) interface for soil loss estimated per grid cells continued.	68

List of Tables

5.1	Estimated Annual Rainfall Erosivity Factor (R) (MJ/ha.mm/hr.)	36
5.2	Size limits of soil texture classification (world soil data set)	37
5.3	The number of grid cells (NPix) and their respective areas calculated from Topographic factor (LS) interface by ILWIS RUSLE 3.0 and their erosion risk categories	42

Acknowledgements

This study would not have been possible without, the fellowship award from the Netherlands Government through the Netherlands Fellowship Program and the genuine support by by Gedeo Zone Department of Water Mines and Energy Resources Development and Zonal Administrative council to participate in competition in general, and wise selection process by Southern Region Government Training Sector in particular. I therefore, extend my heartily thanks to these all institutions.

I am deeply indebted to my supervisor, Dr Tsehai Woldai for his diligence, critical comments and suggestions. His tireless efforts and willingness to help at any time encouraged me very much and deepened my interest in my work. My deep appreciations go to Dr. Paul van Dijk, for his fatherly advise, providing data and offering suggestions during his precious time; prof.Dr. Freek van der Meer for his encouraging advise; Dr. Ernest Schetselaar and Dr. Dhruva Pikha Shrestha for their critical comments and providing data; Dr. David Rossiter for his constructive suggestion and Dr. Abbas Farshad for his attractive approach and constructive suggestions.

I also duty bound to express my thanks to Dr. Tamiru Alemayehu for his encouraging advise and to all friends and fellowship students who have shown interest and afford help in one way or the other.

The full commitment from all my parents, my mother Awade, my wife Mulunesh, all my children and the rest of the family members inspired me throughout the study period. Words are not enough to express my sincere gratitude to all of them.

Last, but first, I deeply thanks God Almighty , who blessed and taking care of me and my family and Who made all these to happen.

Abstract

This research enabled to estimate soil erosion by water in study area (northwest Tabernas); and the erosion process in the area highly depends on *the nature of parent materials (geology), soils (texture, organic matter, structure and permeability), topography, climate (rainfall), cover management and supporting practice*. The general research aim was to estimate the effect of soil erosion on soil loss per year. To reach this goal the following objectives had to be satisfied: computation of rainfall-runoff erosivity factor (R); computation of cover management factor (C); examination of the spatial distribution of slope factors (LS) in terms of their erosion status; and characterization of the major soil types and computation of soil erodibility factor (K).

The two principal erosive agents operating during rainstorms are falling raindrops and flowing water. The energy of falling raindrops is generally applied perpendicular to the soil surface and is primarily responsible for detaching of soil particles while the energy of flowing water is usually applied parallel to surface of soil and it is primarily responsible for transport of soil material. Both raindrops and flowing water are complete erosive agents in themselves, but in one phase of the erosion process they work together. Irregular and often intense rainfalls in this semi-arid region can result in sheet erosion where the slope is low; and rapid erosion (Gully erosion) in areas where the slope is steep and parent materials are soft. The past and on-going neotectonic activities are also the main controlling factors in facilitating the process of soil loss by erosion.

The use of new technologies and science developments such as remote sensing (RS), geographic information systems (GIS), database development have made possible to approach the study of soil erosion. The potential use of NDVI provides a crude estimate of vegetation health and a means of computing land cover factor (C). The Revised Universal Soil Loss Equation (RUSLE) is an easily and widely used computer program that estimates rates of soil erosion caused by rainfall and associated overland flow. Digital Elevation Model (DEM) of study area was used as a source data for ILWIS 3.0 RUSLE Topographic Factor (LS) interface. ILWIS 3.0 RUSLE Topographic Factor (LS) interface has played great role in calculating slope percentage, slope degrees, slope factors (LS) and area per grid cells. Similarly ILWIS 3.11 Academic, Microsoft Excel, WinEdit (Latex), ArcView, Paint and Microsoft PowerPoint were used for data storing, manipulation and analysis, and for displaying maps.

In this research it was observed that soil loss or erosion by water is highly sensitive to slope factors (LS) and equally but less sensitive to rainfall erosivity factor (R), soil erodibility factor (K) and cover management factor (C).

KEYWORDS

Soil loss, Rainfall-runoff erosivity factor, soil erodibility factor, Slope factors, Cover-management factor, support practice factor, Remote Sensing, Geographic Information System, Revised Universal Soil Loss Equation, rainfall (precipitation), Normalized Difference Vegetation Index.

Chapter 1

INTRODUCTION

Environmental Impact Assessment is, in its simplest form, a planning tool that is now generally regarded as an integral component of sound decision making.

- As a planning tool it has both an information gathering and decision making component which provides the decision maker with an objective basis for granting or denying approval for a proposed development [35].
- It is a process, which attempts to identify, predict and assess the likely consequences of proposed development activities.
- It is a planning aid concerned with identifying, predicting and assessing impacts arising from proposed activities such as policies, programmes, plans and development projects which may affect the environment.
- It is a basic tool for the sound assessment of development proposals to determine the potential environmental, social and health effects of a proposed development.

Soil erosion is one form of soil degradation along with soil compaction, low organic matter, loss of soil structure, poor internal drainage, salinisation and soil acidity problems. Soil erosion is a naturally occurring process on all land and it becomes a problem when human activity causes it to occur much faster than under natural conditions. The terms land degradation (soil erosion) and desertification have closer relationship and several attempts to define and describe them have been made by many researchers [57] [9] [27].

The term "desertification" has been interpreted as land degradation (soil erosion) in arid, semi-arid and dry-humid environments and the first worldwide attempts to deal and combat desertification come from the United Nations Conference on desertification organized by UNEP that was held in Nairobi, Kenya, in 1977. There are many definitions and classification systems of desert. A climatic classification is the most widely used system. Perl Meiges (1953), divide desert regions into three categories according to the amount of precipitation that they received. In this widely accepted classification systems, areas with less than 250 millimetres of mean annual rainfall are classified as arid. Arid and extremely arid lands are deserts [58]. Although the Desert of Tabernas is at the limit between arid and semi arid areas, according to UNEP criteria, and on the basis of the annual rainfall of 218 mm it falls under semi-arid climatic zone [54]. The application of other widely used climatic classifications [56] also allow to identify the area as the arid, therefore, this classification has led to consider the Desert of Tabernas as an area belonging to the arid Mediterranean environments [50]. The classification category, which is based on the rainfall limits, corresponds approximately to changes in vegetation, soil and drainage [29].

According to various estimates, approximately one-fourth to one-third of the earth's land surface is desert [58] [61] and the livelihoods of over one billion people in more than 100 countries are also jeopardised by desertification [58].

Soil erosion (land degradation) is an important social and economic problem and an essential factor in assessing ecosystem health and function. It is a process of deterioration of the fertile soils and loss of biological and economic productivity in different forms that leads to a situation of unbalanced environmental conditions. Soil erosion is a fundamental and complex natural process that depends mainly on rainfall erosivity, soil erodibility, land cover and topography and is strongly modified (generally increased) by human activities such as land clearance, agriculture (ploughing, irrigation, grazing), forestry, construction, surface mining and urbanization. In general it is estimated that human activities have degraded some 15 percent (2000 million ha) of the earth's land surface between latitudes 72 degree North and 57 degree South (FAO). Slightly over half of this is a result of human-induced water erosion and about a third is due to wind erosion (both leading to loss of topsoil), with most of the balance being the result of chemical and physical deterioration.

Soil erosion is a very widespread phenomenon and is usually irreversible. Erosion, the detachment of particles of soil and surface sediments and rocks, occurs by hydrological (fluvial) processes of sheet erosion, rill and gully erosion, and through mass wasting and the action of wind (sediment geochemistry and stratigraphy; stream sediment storage and load; wind erosion). Erosion both fluvial and eolian (wind) is generally greatest in arid and semi-arid regions, where soil is poorly developed and vegetation provides relatively little protection. Where land use causes soil disturbance, erosion may increase greatly above natural rates. In uplands, the rate of soil and sediment erosion approaches that of denudation (the lowering of the earth's surface by erosion processes). In many areas, however, the storage of eroded sediment on hill slopes of lower inclination, in bottom lands, and in lakes and reservoirs leads to rates of stream sediment transport much lower than the rate of denudation.

When runoff occurs, less water enters the ground, thus reducing crop productivity and once the nutrient rich surface soil has been lost, the ability to sustain plant growth is severely reduced and increased runoff from the more impermeable subsoil results in a decrease in plant available water and the diversity and abundance of soil organisms. Further more, erosion brings various associated "off-site" problems, including *reduced water quality from increased sediment loads and poorer air quality due to dust*. The semi-arid Mediterranean environments are one of the geographic areas affected by soil erosion and their causes and extent has been the object of study for more than a decade.

The application and integration of multi-sources of information represent a major goal to achieve more satisfactory results in the assessment of many environmental issues. The use of new technologies and science developments such as remote sensing, geographic information systems, field data collection, database development have made it possible to approach the study of soil erosion from multi-disciplinary perspective.

The actions of planning and managing the use of natural resources are of primary importance nowadays to integrate and focus the generation of geo-information to develop or improve the policies for a sustainable development. To achieve this, in the case of semi-arid Mediterranean environments, the requirements of comprehensive and accurate information about the spatial distribution and dynamics of soil erosion processes is one of the priorities of special interest in order to formulate the policies for an integrated environmental planning.

The desert of Tabernas, which belongs to the province of Almeria in southeast Spain, was selected to conduct the assessment of spatial distribution of soil erosion. The approach that will be followed to assess those indicators is based on the use of remote sensing, geographic information system and ancillary data that which will support to estimate soil loss by using Revised Universal Soil Loss Equation (RUSLE) modelling and ILWIS 3.0 RUSLE Topographic Factor (LS) interface.

1.1 ENVIRONMENTAL PROBLEMS IN THE STUDY AREA

The current study area, Tabernas, is located at about 37 km north of the city Almeria in South-eastern Spain. With its mean annual precipitation of 248 mm, it is said to be the only true desert in the whole of Europe fulfilling the criteria of a desert. Many of the processes of desertification involve past and on going geological and geomorphologic processes.

Desertification around Tabernas is not a recent event, but something that started in the geologic past [32]. The extreme climatic nature as a result of human activities makes the area particularly sensitive to environmental changes. There are many environmental problems that can be associated with the desertification processes of the study area. These include, soil degradation, depletion and contamination of surface and underground water, landscape deterioration and loss of bio-diversity as major ones. Seasonal drought and topographic restrictions can be given as main reasons for the difficulty of maintaining agricultural activity [50]. Although lots of them are natural and reversal is difficult, still many are aggravated by human interference. Uncontrolled land use practices, such as over cultivation and poorly drained irrigation, over grazing, mining, quarrying, over pumping of the groundwater resources, deforestation and etc. lead to the environmental crises. Such processes aggravate the drought problems and the repeated drought increases the risk of desertification. The term land includes land and local water resources, the land surface and its natural vegetation. It is important to notice that this definition, attributes the cause of land degradation to natural processes and human activities are introduced as another factor. Land degradation (soil erosion) can be defined from another perspective [9], as "alterations to all aspects of the natural (or biophysical) environment by human actions, to the detriment of vegetation, soils, landforms, water (surface and subsurface) and ecosystems". The Desert of Tabernas is a typical example of and probably the most affected by such desertification and land degradation (soil erosion) processes. The climatic nature of the area, which is a result of many combined factors, is one of the most important factors influencing the environment. A study done for the whole province of Almeria indicates that torrential rains supply only 18 cm precipitation/year. Normally up to 95% of the total precipitation is lost by evaporation so that groundwater replenishment cannot be meteorically maintained [63].

In the study area, soil erosion is the most critical problem with the nature of the rock type and mechanical weathering as the main responsible agent for the badlands morphology. The soft nature of the rocks (marl, clay and sandstone) in association with dynamic tectonic process has facilitated the erosion process. Surface erosion has considerable impact. The inclined and tectonized nature of the sedimentary bed and the lack of vegetation cover have aggravated the high surface runoff. These result in a minimum role of soil moisture and a low ground water recharge. The geologic setting of the basin and the alternating wetting and extreme drying have also facilitated mechanical weathering, rock fall and debris flow. As it realized in the field, active mass wasting occurs in many places of the study area.

Apart from the mechanical weathering and erosion, the nature of the underlying rocks with dry climatic situation has given rise to salt weathering [3]. The weathering of the bedrock might result in the precipitation of salt because of mixing of different salt solutions. Hydration and thermal expansion of salt is also expected to take place. Salinity, which is also aggravated by human action, as irrigation intensified, is another main process that affects the environmental quality of the study area.

Other than the above-mentioned human influences, the age of human development endeavours has also created its toll on the quality of the environment. Infrastructure developments, tourism, mining and associated improper utilization of resources have exerted their pressure. The badlands are the attractions for the film making activity in the desert. As a result there are numerous inter-valley access roads and villages that have been built in the pristine environment. These

and the influx of many tourists and associated activities have to a certain extent also added to the deterioration of the environmental quality.

1.2 PREVIOUS ACTIVITIES

Since 1989 the European Community has established and funded a number of international programmes of research to address the issues of desertification or land degradation and the increasing demand on water resources across southern Europe. Mediterranean Land Use and Desertification (MEDALUS) [41] is one of the projects in this programme with the main objectives of:

- **Field studies of soil erosion and vegetation growth;**
- **Climate variability and climate change;**
- **Computer modelling of river basin response to change; and**
- **Socio-economic issues related to land degradation processes.**

Also an important component is the identification of possible mechanisms for mitigating land degradation effects in the context of Mediterranean Europe. Since its start (MEDALUS) in 1991, there were three phases to the project and the third of which ended in June 1999.

The ongoing EU environmental project, contract no.ERBIC18-CT98-0290 entitled "Euro-Latin American Network for Environmental Assessment and Monitoring (ELANEM)" is aimed on identifying and assessing quantitative indicator and indices to measure environmental quality in various study area of Europe and Latin America, including the above mentioned Desert of Tabernas. It started on May 1st 1999 and ended in April 31st 2002. The research is being carried out in ten study areas of eight countries in Europe and Latin America, covering a wide spectrum of environmental conditions, from both the natural and human points of view. The approach is interdisciplinary; scientists working in the project come from the earth sciences, ecology, geography, oceanography, engineering, economics and social sciences. The Geological Survey Division of ITC is one of the eight partners [17]. Again, this work was carried out in target areas, all of which are sensitive to degradation; they were the Guadalentn-Segura Basin in Spain; the Agri Basin in Italy; the inner-lower Alentejo region in Portugal; and the island of Lesbos in Greece.

The ELANEM project partners have suggested an indicator based approach methodology [7] and a Pressure-State-response framework [34] [1] [53] to achieve the goal of evaluating the environmental quality in the different pilot areas. They are based on the identification and assessment of a series of environmental indicators that permit to measure the pressure exerted, the state of and the policies for managing the environment and its natural resources. Environmental functions like degree of naturalness support of services and sink of wastes are evaluated through specific indicators. The role of remote sensing and geographic information systems as well as field data collection and laboratory analysis has been relevant to their construction and evaluation.

As part of the evaluation of the environmental quality of the Tabernas area, previous work has been carried out under the ELANEM project. Aspects such as land use, land cover and their changes through the last 50 years [3], Mapping salinity using multispectral and hyperspectral data in Tabernas, south east Spain [36] and definition of environmental units [50], evaluation of the degree of naturalness [4], soil moisture measurements and desert like features mapping [?] and assessment of morphodynamic processes and soil pollution as indicators of land degradation, a case study in the Tabernas area, southeastern Spain [47] have been studied. In each of these works only one specific type of remotely sensed data has been employed (or aerial photographs or hyperspectral imagery or satellite imagery). The capabilities and limitations of different and more recent type of sensors, as well as possibilities of data integration have not yet been explored.

The aspects that have been investigated in the previous works are related to a certain extent to the land cover change detection and land degradation problem that affects the area of Tabernas. The intrinsic environmental conditions and characteristics (geology, climate, soils, morpho-dynamic processes and vegetation) and the human interference with natural environment have resulted in:

- Inadequate land management;
- Intensive changes in recent years of the land use and land cover;
- Mining and quarrying;
- Soil contamination and soil compaction; and
- Over pumping of groundwater and overgrazing.

These are the main aspects that have to be understood in order to evaluate the state and probably infer the future trends of land degradation (soil erosion) process.

1.3 RESEARCH OBJECTIVES

The main objectives of the research are:

- To understand the several dynamic processes responsible for environmental degradation (soil erosion), which is happening through physical and biological stress. The guide-line of this investigation is to determine the natural responsibility in soil erosion.
- To assess and monitor environmental spatial changes of erosion focusing on landform (topography).
- To adapt current erosion models for use in field level scales.
- To estimate natural or geological soil erosion (loss) by water.
- To evaluate the potentials and limitations of remotely sensed data e.g. aerial photographs, Landsat imagery to map erosion-affected areas.

1.4 IMPORTANCE OF THE RESEARCH

This work has helped in the analysis and assessment of the environmental quality of natural resources and can assist in decision making for land use planning in the study area. It also provides the possibility of generating other descriptive, diagnostic and prescriptive maps. The result of spatial change detection results and other related findings in this work helped to identify the main soil erosion (land degradation) processes that taking place in the study area (northwest of Tabernas). The results have applicability not only in the study area but particularly too much of the Mediterranean climate areas.

1.5 METHODOLOGY

This section describes the operational workflow that has been followed during the development of this research. Particular details about the satellite image processing aspects, NDVI classification, rainfall data acquisition, rainfall-runoff erosivity factor (R) estimation, soil data acquisition, soil erodibility factor (K) estimation, cover management factor (C) estimation, slope length and slope steepness factor (LS) estimation, conservation practice factor (P) estimation, soil loss calculation and result evaluation are presented in separate chapters. A flow chart of the operational aspect is presented in Figure 1.1.

In addition to the above mentioned research methodology, steps undertaken during this work include a literature review on area of study, on soil erosion , on the use of remotely sensed data

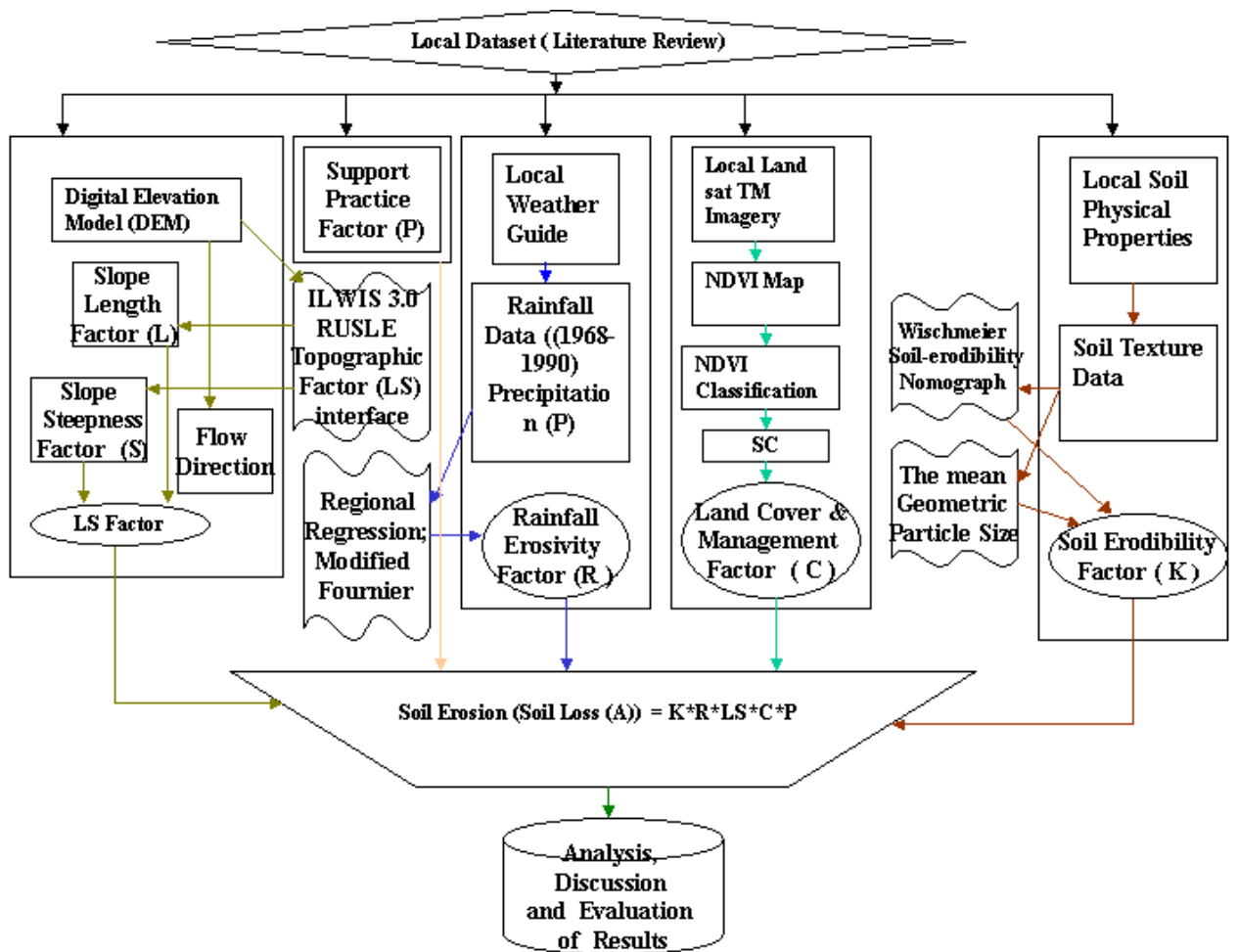


Figure 1.1: Operational Flow Chart.

and on the application of Revised Universal Soil Loss Equation (RUSLE) modelling in soil erosion. An extensive search and review of all previous studies and works carried out in the Tabernas area was done via the Internet. The rest procedures that have been followed during this thesis are explained fully in chapter or section.

1.6 RESEARCH MOTIVATIONS

The main issues for this research include:

- Are there any landform and soil erosion (land degradation) interaction that can be detected and modelled to assess soil erosion in the study area?
- Is there any link among the geology, geomorphology, climate, land cover and soil erosion?

1.7 HYPOTHESIS

- There is spatial variation in the environmental quality that can be detected using remotely sensed data and various records.
- The degree of deterioration of the environmental quality is not uniform throughout the study area.
- The natural influences are determining factors for the soil erosion process in the study area (northwest of Tabernas).
- There is strong relationship between the geological processes and erosion.
- DEM might be helpful in designing slope factors (LS) and also to determine the erosion flow direction.
- Revised universal Soil Loss Equation (RUSLE) modelling may be helpful in calibrating soil loss.
- Landsat TM imagery may be useful for the determination of land cover factor (C).
- Due to their spatial resolution and the possibility of getting wide coverage, aerial photographs can give better results in determining the geomorphology (landform).
- The zooming in facility and the possibility of image overlaying in a GIS environment can give better interpretation results.

1.8 RESEARCH OUTLINE

The research report is organized in seven chapters and followed by sections and subsections, which defined as follows:

- Chapter two gives a short description of the study area with respect to its location, climate, geomorphologic, soil and landcover/use;
- In chapter three, the geology and structure of the area and their relation with the environment are discussed;
- In chapter four, Material, Research methods and Techniques are discussed;
- Chapter five contains the general description of soil erosion and spatial estimation of soil erosion using RUSLE modelling;
- Chapter six includes the overall result analysis and discussion; and
- Chapter seven is followed by conclusions and recommendations.

Chapter 2

DESCRIPTION OF THE STUDY AREA

2.1 LOCATIONS AND ACCESS

The study area (northwest of Tabernas) as shown in Figure 2.1, is located 37 km north of the city of Almeria, in southeast Spain. The study area covers a total area of 300ha or 3km² and bounded by UTM zones: X1: 551000.00, Y1: 4103000.00; and X2: 553000.00, Y2: 4104500.00.



Figure 2.1: Location map of the Tabernas Basin (the study area).

The town of Tabernas is the largest municipality in the study area and it is located at 400 m.a.s.l and has a population of 4080 [3]. The city of Almeria, with a population of 145,000 is located 37 km south of Tabernas town. The city of Granada, with a population of 700,000 is located at about 150km NW of Tabernas. Around the Tabernas areas there are smaller villages such as Manicas, Níjar, Lucainena de las Torres, Gálor, Turrias, Los yesos, Sorbas, Las Alcubillas and Gergal. Except for the rugged mountains parts, most of the areas are accessible during the dry period. Road transport from Almeria, through the Carretera Nacional

340, is the main means of access in the area.

The landscape of Tabernas is hilly with a drainage network flowing towards *Tabernas Stream*, which in turn flows in the southwest direction to join a big river called *aqua (Rio Aqua)* that flows on southwards to the *Mediterranean Sea*.

2.2 CLIMATE

Tabernas Basin has thermo-Mediterranean semi-arid climate, with mean annual temperature of 17.9 °C and average minimum temperature of 4.1 °C in the coldest month and an average of 34 °C in the hottest month, and the average daily amplitudes is 13.7 °C in summer. Rainfall events are produced by rain bearing fronts, associated with the Atlantic Ocean, coming from the west, principally in the cold season. The pronounced regional semi-arid climate in the SE Iberian Peninsula is determined by its geographical location, in the rainfall shadow of the main Betic ranges and the proximity of northern Africa [24]. The mountains of the Sierras Alhamilla and Los Filabres constitute natural barriers for the winds and humid conditions that come from the Mediterranean Sea.

The rainfall days are concentrated in two periods; *Spring and Fall (Autumn)*, and the maximum rainfalls are recorded in *October and December*. In the autumn, rainfall is associated with incoming fronts from the Mediterranean Sea, which sometimes results in storms and torrential rains. Torrential rains supply only 18 cm precipitation/year averaged over 25 years and they usually falls in only a few days, leaving the rest of the year completely dry.

Precipitation over the Almeria region is influenced both by the December North-Atlantic Oscillation and by the October Southern Oscillation [26]. According to a 25 years meteorological record of nearby Tabernas station the area has a mean annual precipitation of 218 mm, which ranges from 115 to 431 mm with the rainy days varying from 25 to 55 and an average of rain days of 37 [54]; only 6% of the rainfall events yield more than 20 mm and only 0.7% exceeds 50 mm/day. The maximum-recorded rainfall intensity at the on-site meteorological station during the year 1992-93 was 85.2 mm/h during 5.7 minutes [41].

In response to the interest in problems of aridity and desertification, a map showing the world distribution of deserts was produced in 1977 [59]. For this map, arid regions were delimited partly on the basis of aridity indices and partly from considerations of all available data on soil, relief and vegetation. The degree of bio-climatic aridity was defined by the ratio of the mean annual precipitation **P** to the mean annual potential evapotranspiration **ETP** [11].

Four main classes of aridity were defined as follows [59]:

1. The hyper arid zone ($P/ETP > 0.03$)
2. The arid zone ($0.03 < P/EPT < 0.2$)
3. The semi-arid zone ($0.2 < P/ETP < 0.5$)
4. The sub humid zone ($0.5 < P/ETP < 0.75$)

As cited by Palacio (2002) [60] Tabernas, with mean annual precipitation of 218 mm and the mean potential evapotranspiration ETP 779.5 mm has the ratio to P/ETP about 0.28, which according to the classification of [11] corresponds to a semi-arid zone. The graph and table that show Tabernas monthly precipitation, potential evapotranspiration and temperature for year 1968-1990 are presented in Figure 2.2.

The importance of defining the climate of Tabernas area is due to the fact that it controls the soil and landscape development as well as the dynamic of the soil erosion processes that take place through out the time.

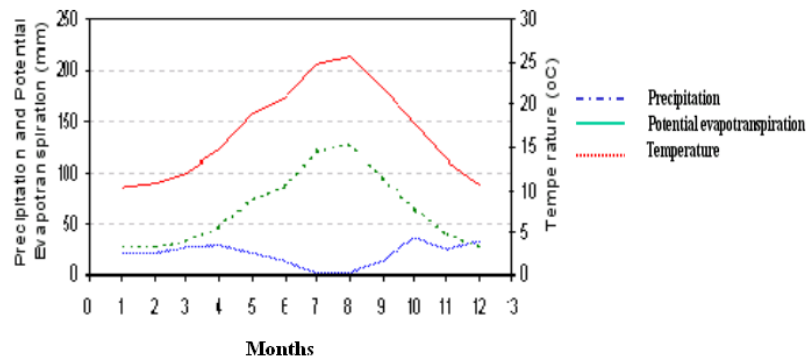


Figure 2.2: Monthly Precipitation, potential evapotranspiration and temperature in Tabernas area.

1

2.3 GEOMORPHOLOGY

The geomorphology of the province of Almeria is to a great extent controlled by geological structures. Highs in the regional relief (600-2000m) coincide with axial culminations in the inliers of refolded basement rocks of the sierra de los Filabrides, Alhamilla and Estancias. The topographic lows (less than 600m) are occupied by the Neogene sedimentary rocks, that form intermontane basins between the basement highs [63]. The Tabernas Basin, where the study area is located, is a structural depression in the alpine nappes of the Betic Cordillera fold belt of southern Spain, which in turn is the western continuation of the alpine orogeny. The stratigraphic series (highly bio-turbated marls) give rise to badlands. Badlands development is related to the episodic tectonic uplift that has been active during the quaternary. The Tabernas badlands are the most extensive ones in southeastern Spain [54]. The second highest peak of Spain, with an altitude of 3478 m at Muichen in the Sierra Nevada mountain chain, is located N-W of the study area and S-E of Granada [3]. The two most important and closer mountain chains are the sierra de Alhamilla, with a peak elevation of 1387m at Colativi, located south of Tabernas and the Sierra de los Filabres, with a peak elevation of 2168m at the Centro Astronomico Hispano-Aluman. The doubly plunging anticlinal structure of the Sierra de Alhamilla chain is about 25 km long. The Sierra de los Filabres is a very wide anticlinorium that is concerned with the Sierra Nevada. In the desert of Tabernas the geomorphologic characteristics of the area are highly controlled by the NW-SE and E-W trending mountain chains that form a topographic strike and the basins developed between them. The same geological forces those were responsible for the formations of the mountain chains were also responsible for the creation of the low-lying basins [32] [63]. Dissected and denudation morphology in the mountain chains and depositional land forms in the valleys,

¹T: monthly temperature; P: monthly precipitation and P.E.T: monthly potential evapotranspiration

with wide canyons and numerous stream channels are typical geomorphologic features of the area. The dissected lunar type landform in combination with the arid climatic condition has become an attraction for film production companies.

According to many studies carried out in the study area (northwest of Tabernas) in general, and in Tabernas in particular the area is divided into five environmental units [4] [3]:

- Mountain, piedmont, Hilland, Valley and Badlands.
- The Mountains: A mountain is an elevated, rugged land portion characterized by an important relative height and steep slopes in relation to lower-lying surrounding landscape units, and by an important internal dissection, generating high relief energy [33]. The high grounds of the southern extension of the Sierra de los Filabres in the north and the Sierra Alhamilla in the south with an altitude ranging from 750 to 1317 meters and that are mainly composed of basement rocks, with slope greater than 30 percent are grouped into the mountain environment.
- The Piedmonts: A piedmont is a sloping land portion lying at the foot of a mountain, hilland or plateau [33]. The piedmont areas are highly affected by tectonics and are dissected by the incision of valleys. Most parts are sloping 8 to 16 percent and have an altitudinal range of 500 to 750 m. Most of the piedmonts are covered by Gorgonian sediments and recent colluvial cover derived from the mountains
- The Hillands: A hilland is a rugged land portion characterized by the repetition of high hills, generally elongated, with uneven summit heights, separated by a moderately dense hydrographic network [33]. The hillands consist of the Tortonian marls, sandstones and conglomerate. They are dissected by several dry drainage lines locally named as Ramblas. The dissection result the removal of the top layer and exposure of underlying materials leading to the spatial variety of the surface materials. These units have an average elevation ranging from 500 to 750 m and in most cases have slope of more than 30 percent.
- Badlands: The badlands are found in the south-western part of the Tabernas area and illustrated in Figure 2.3. They are extremely dry, dissected and have soft Neogene sedimentary covers, mainly composed of marls, clay, sandstone and conglomerates.



Figure 2.3: Badlands geomorphology of the Tabernas area [20].

- Valleys: The valleys constitute low-lying Quaternary sediments covered plains in the central part of Tabernas Basin and wide intermountain valleys towards the northern parts. They represent the recharge zones with better moisture content, thick and relative fertile soils.

2.4 SOILS

The soil characteristics of the Tabernas Desert are strongly controlled and influenced by the nature of the parent materials and the geologic forces prevailing in the area. The past and recent geologic processes, such as transgression and regression of the sea, the orogenic movement and etc. are manifested in the type and nature of the soils. High rates of soil erosion also contribute to the shallow development of soil horizons [54]. The dryness that also slows the process of weathering, together with the type of parent materials contribute to the evolution of sandy textured soils [39]. Variations in the soil properties depend mostly on the lithology from where soils are developed.

The parent materials are a hard and are developed from siliceous materials, micaschists and quartzites from the Nevado Filabride Complex. They are Petrographically identified as siliceous and calcareous; and composed dominantly by sand size particles that range in % from 2.35-81.85; silt particles range in % from 1.56-74.64; and clay particles range in % from 2.69-58.79 [36]. Conglomerate, sandstone, marls, micaschist, and quartzites are the dominant rock types in the area. Bulk mineralogical compositions are quartz, mica (muscovite and biotite), feldspar, calcite, garnet, gypsum, psammite, plagioclase and pyroxene. Very scarce fissures form the only visible porosity. Some joints of either stratigraphic or tectonic origin are filled with veins of a few centimetres thick of crystalline calcite (esparite), which when exposed by erosion, break down in gravel-size fragments that partially cover pediments and channels.

Climatic conditions of high aridity, morphologic and micromorphologic features (slope) are also factors that influence the soil development. The dominant soil groups mapped by the Ministerio de Agricultura Pesca Y Alimentacion (1987) are Lithosols, Fluvisols, Xerosols, yermosols, Cambisols, Luvisols and Solonchaks. Determined from the the soil Map of the World (FAO-UNESCO, 1974) and was published in a 1:100,000 scaled soil map for Tabernas (Mapa de Suelos Tabernas-1030). The soils in general are very shallow to shallow (50 cm depth), except along the valleys and occasionally on the piedmonts. Soil depth can reach up to 1 meter along valleys, especially in agricultural areas. Soils in the steeper slopes are mostly derived from the weathering of the exposed bedrocks, while along the valleys, they consist of irregular deposits of materials coming from the surrounding Mountains (Sierra de los Filabres and Sierra Alhamilla) and Hillands brought down by flash floods. Soil texture is commonly sandy loam to loamy sand with more than 40% coarse fragments on the surface [39]. Soil colour ranges from 7.5YR 4/1 (dark gray) to 5Y 8/6 (Yellow) [39].

Formation of crusts on the surface and accumulation of salts are found mostly along the valleys. Soils are neutral to strongly alkaline with PH value of 7 to 9. Saline soils occur along the valleys with electrical conductivity values of more than 2 dS/m [39]. Soil temperature regime for the area is thermic and soil moisture regime is aridic (Tabernas-1030, Mapa de Suelos, 1987).

According to Soil Taxonomy (USDA, 1998) ochric epipedon and cambic horizon are the common diagnostic horizons in the area. Calcic horizon also occurs in small areas and fluventic properties are manifested by large areas. Ochric, cambic and calcic are the main diagnostic horizons, whereas salic, takyric and yermic occur locally (FAO, 1998). Soils in the Hillands and Piedmonts lack diagnostic horizons other than ochric epipedon. These soils are very shallow with lithic contact within 50 cm from the surface, consequently fitting into the classification of Lithic Torriorthents; loamy-skeletal, mixed, non-acid and thermic [39]. According to the USDA Soil taxonomy (1998) deeper soils in the Piedmonts could qualify into loamy-skeletal, mixed, calcareous and thermic Typic Torriorthents. In the valleys, soils are

are classified as Fluventic Haplocambids, with fine-loamy, mixed, calcareous, thermic differentiae at the family level. Towards the upper terraces, soils belong to fine-silty, mixed, calcareous, thermic Typic Haplocambids for Soil Taxonomy (USDA, 1998).

In general five taxonomic units with their correspondent soil associations and guidelines presented for soils of study area have been described as follows [12] [18]:

- Lithosols: They are well distributed in the study area but the best locations are the high and steep lands forming part of different associations. They are soils with low evolution and the depth is limited by the bedrock at about 10 cm from the surface. Predominantly, they are developed from the weathering of siliceous and calcareous rocks.
- Regosols: They are formed from unconsolidated materials, but not from recent ones. They are developed from either siliceous or calcareous rocks forming Calcaric regosols and Eutric calcaric regosols respectively; and with the Lithosolic regosols are the most common associations in the area.
- Lithosolic Regosols: They are developed from siliceous materials, micaschists and quartzites from the Nevado Filabride complex.
- Calcaric Regosols: Are one of the most abundant soil type. The parent materials are generally calcareous rocks, conglomerates and rocks from the Nevado Filabride Complex, such as mica schists and quartzites. They have abundant stones and the slope ranges from moderately tilted to steep terrain.
- Eutric Regosols: They are developed from schists and quartzites with moderate to highly steep slopes. They are well-drained soils, present a stoniness of less than 50% and have an average depth of less than 20 cm.

2.5 LAND COVER

One of the main indicators of changes in the study area is land cover. The dominant land covers of the area are bush and grass cover with and without trees. Next to the bush and grass cover is the diminishing seasonal cultivation followed by non-natural vegetation [3].

The presence of scanty bush and grass cover within dissected bad land make the cover of the area sparse bush and grass cover. The southern basement and the limestone rock cover area contain relatively denser vegetation cover than the northern basement and the area covered by other Neogene sediments.

2.5.1 CHANGES IN LAND COVER

In desert of Tabernas no significant visual change that can be detected on aerial photos has taken place in the hilly and mountainous areas covered by bush and grass, commonly known as "*matorral*" [3]. Many changes have taken place in the highly used valleys, where there has been human involvement. The largest change was the decrease in seasonal crop (SC). This class has lost a total of 2652 hectares of land followed by the "*Sparse Bush Cover with Trees (SBCT)*" class that lost a total of 306 hectares [3]. Similarly, the natural tree cover on the Sierra Alhamilla has lost a total area of 235 hectares and the "*Dense Bush and Grass Cover (DBGC)*" about 97 hectares. On the contrary, there was dramatic increase in the tree plantation cover (TPC), which had grown by more than 4200%, covering an area of 426 hectares at present from the 10 hectares covered in 1956. The second largest increment, percentage wise, is the growth in the Non-Natural Vegetation (NNV) class. This class represents any kind of permanent tree plantation that has been cultivated, such as olive, almond, citrus trees, etc [3].

2.6 LAND USE

Agriculture (cereals and irrigated crops), tourism (the movie and entertainment industry), mining (gypsum, marble, gravel and sand) and hunting are the four main land use types. In the past, pasture was one of the main land use types, which have diminished at present [50]. Part of the area is protected by the government and individuals to protect the ecosystem and as hunting ground (from the master plan of Tabernas).

After the dying (vanishing) type of land use of pasture, diminishing type of land use is dry farming. Dry agriculture is a difficult activity in this area because of climatic (seasonal drought) and topographic conditions [50].

2.6.1 CHANGES IN LAND USE

Land use in the Desert of Tabernas is the most dynamic environmental element that has undergone a change to the extent of visible affecting the environmental quality. The area has a long history of economic and social interactions. Irrigation practices in Andalucia have a long history. Much of the regions elaborate irrigation construction dates from the Muslim period [3].

Among the land use classes of areas features, the reduction of the dry farming (DF) practices is the biggest change that was observed. From year 1956 to 2000, the total of dry farm shrink from 7957 hectares to 5351 hectares, a reduction of 32percent. On the other hand, the irrigated trees, Olive (IRTO) class has shown a big increase of 1337 hectares in 2000, which in 1956 was 400 hectares and this shows an increase of three folds (345%). The change in irrigated tree (Almond), is also significant. There was an increase of four folds (401%) in year 2000, this means that the total area coverage which was 196 hectares in 1956 increased to 786 hectares in 2000. The mining activity has also grown much. Forest (F) class also has shown a considerable increase due to the pine tree plantation on the mountains and the eucalyptus tree plantations in the valleys. Similar to area features, changes have occurred in the linear and point type land use features. The landscape that was affected by constructing access road was 61.55 km in length with a total area of 38 hectares in 1950, where as in 2000 the length of access road reached 115.9 km and covered the total area of 63 hectares. This amount does not include the roadside cuts and the buffer zone that is affected by the road for far seeing [3].

The other fast growing linear features that considerably affect the landscape are the power transmission line. In 1950, there was 23 km of 66 KV power transmission lines, while in 2000; it was 35.4 km of power transmission lines, with the improvement of the type of power transmission lines to high-tension type. Apart from the high-tension line improvement, intricate power transmission lines of 45, 15 and lower KV lines have been extended as the need for additional power for water pumping and other agro-industrial applications increased around the drip irrigated Olive and Almond farms [3].

The socio-economic trends and the environmental quality change can be also detected by the trend in the growth of the water points. The number of reservoirs has increased from 13 or 0.05/km² in 1950 to 119 or 0.43/km² in 2000. Similarly, a number of water wells grown from 8 or 0.03/Km² to 68 or 0.25/km² in 2000. The overall increase in water point distribution was 730% from 1950 to the 2000 and 165% from 1981 to 2000. Most of the changes were occurred around the olive and almond irrigation farms [3].

2.7 GEOLOGIC PROCESSES AND LAND DEGRADATION

According to the study carried out [47] from total of 26480.7 ha in study area 5831 ha or 22.02 percent affected by different types of land degradation in 1956. The degradation of land by erosion highly observed in the unit formed by marls, sandstones and conglomerates and nearly 51 percent of it affected by soil erosion. In those geologic formations, sheet and rill erosion presents an increase from 1020 ha in the year 1956 to 1156 ha in 1995. Another process that presents significant increment in extent through time in this unit is the gully and sheet erosion. They shown an increase from 23.48 ha in 1956 to 282.2 in 1995 [47]. This fact also related to the increase in the areas that affected by sheet and gully erosion as individual process.

Another unit with high susceptibility to different morphodynamic process is the graphitic schist and quartzite of the Nevado Filabride Complex. The foliation planes in this unit represents discontinuities and the sandy to coarse nature of the scarce soils that are developed from these materials favour the action of the erosive agents. In this unit Processes such as rill erosion present a high increase of 78.36 ha from the year 1956 to 1995 [47].

As it is mentioned above from total 26480.7 ha of study areas of that particular time, sheet erosion covers nearly 10% of the study area. Areas with a combination of rill and sheet erosion occupy 5%. Areas affected by solution process occupy 2.81%. Areas affected by gully erosion occupy 1.37% and those of gully mixed with sheet erosion occupy 0.1% [47]

In 1981 the evolution shows an increase from 5831 in 1956 to 6167.04 in 1981 that represents 23.29% of the total area. It was detected an increase of 76.52 ha, with respect to 1956, in the area affected by gully erosion, which correspond to 0.29%. Areas of combination of rill and sheet erosion present an increase of 77.56 ha, which corresponds to 0.3%. Areas affected by gully and sheet erosion show an increase of 27.88 ha that represents 0.1%. An increase in the areas affected by rill erosion from 107.88 ha in 1956 to 175.44 ha in 1981, represents 0.25% of the total area [47].

In 1995 the evolution shows an overall decrease from 6167.04 ha in 1981 to 6156.6 ha in 1995, that represents 10.44 ha or 0.04 percent less than that of the affected area in 1981. And according to this report areas affected by combination of rill and sheet erosion increased with respect to the year 1981 from 1410.84 ha to 1731.64 ha, which represents an increase of 320.8 ha or 1.21%. The areas of a combination of gully and sheet erosion represents an increase from 0.2% in 1981 to 3.36% in 1995 [47].

On the other hand the salinization crisis presents the extension of area coverage of 77.02 ha that represents 0.29 percent of the study area [47].

2.8 INFRASTRUCTURE DEVELOPMENT (ROAD)

Despite the deteriorating environmental conditions, infrastructure development in the area has been increased. Intricate access roads, most of them asphalt, have been built to connect small towns, farm villages and farms too. At present there is a total length of 112 km asphalt road of more than six meters width and about 20 km gravel roads [3]. This accounts for about 280 meters of asphalt road per km² of area.

Chapter 3

GEOLOGY AND STRUCTURE

The Tabernas basin is located in the zone of continental convergence of the African and European plates that brought to the development of the Betic cordilleras. The Betic Cordillera of southern Spain forms the northern arms of an arc-shaped mountain belt that continues across the Strait of Gibraltar in the Rif Mountains of Morocco, surrounding the western end of the Mediterranean known as the Alboran Sea.

The Betic Cordillera is commonly divided into an External zone to the north and an Internal (or Betic) zone to the south. The Betic Cordillera formed at the southern margin of the Iberian plate that cratonized during the Hercynian orogeny in Late Paleozoic times. The Hercynian is overlain by Triassic to early Tertiary supracrustal, which deformed during the Miocene to form the external zone of the Betic cordillera. The external zone was subsequently overthrust by the metamorphic nappe complexes of the internal zone. The external zone consists of non-metamorphic Mesozoic and Tertiary sediments deposited in basinal (sub-betic) and shelf (pr-betic) environments on the former southern margin of Iberia. These rocks were strongly shortened by thin-skinned thrusting and folding during the Miocene [23] [8] [2]. The internal or Betic zone to the south is made up of Paleozoic and Mesozoic rocks, most of which have been penetratively deformed under a variety of metamorphic conditions and are now exposed in elongate ranges typically 15 to 30 km wide, trending roughly parallel to the belt as a whole. These ranges are separated by intramontane basins containing a highly variable record of continental and marine sediments of Neogene and quaternary age. The Internal zone is built of a stack of three complexes derived from a Permo-Triassic cover sequence and a Paleozoic-Precambrian basement. The three-nappe complexes are not readily differentiated on the basis of their lithostratigraphy, but rather on their characteristic mineral assemblages that indicate differences in metamorphic history as a result of their distinct early anti-clockwise PT (pressure and temperature) paths of burial and uplift during the alpine orogenic cycle.

The nappe complexes in ascending order are presented in Figure 3.1 and listed as follows:

1. The Nevado-Filabride Complex;
2. The Alpujarride Complex; and
3. The Malaguide Complex.

The internal zone of the Betic Cordillera is only a small part of the Alboran domain, and until the end of Tortonian, the internal Betic Cordillera would not have been obviously distinguishable from the rest of the Alboran Domain: the whole region consisted of elongate mountainous islands surrounded by marine basins. From Messinian time onward the Betic cordillera was progressively uplifted, whereas the present Alboran Sea continued to subside. During this period the whole region was affected by a combination of strike-slip and

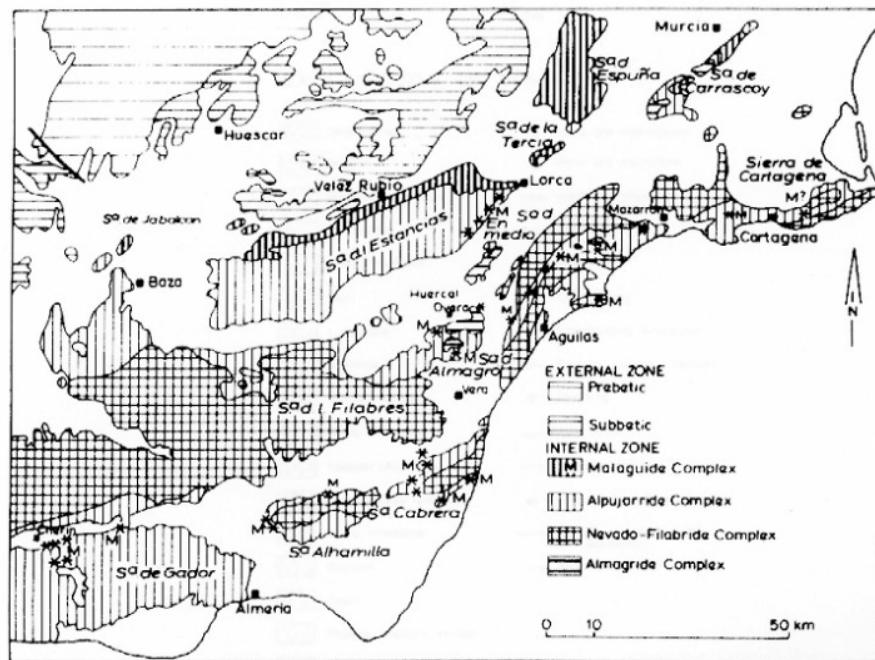


Figure 3.1: Geological Setting of the Betic Cordilleras [63].

compressional tectonics [62]. The Neogene basin sediments were considered to be post tectonic [16].

3.1 METAMORPHIC ROCKS OF THE BETIC ZONE

The crustal rocks in the Betic zone constitute a large number of tectonic units classically grouped in to three tectonic complexes. These are in ascending order, the Nevado-Filabride Complex, the Alpujarride Complex and the Malaguide Complex (see Figure 3.1). These Complexes are distinguished on the basis of a variety of field criteria, including the lithological and metamorphic characteristics of the rocks involved. The metamorphic grade decrease upward across the complexes and the present contacts are largely post-metamorphic. The Nevado-Filabride rocks are pervasively metamorphosed to high -green schist or amphibolite facies. Alpujarride rocks for the most part show low metamorphic grade, although they locally reach upper amphibolite to granulite facies, particularly in the vicinity of the Ronda peridotite; and the Malaguide rocks are almost unmetamorphosed.

3.2 NEVADO-FILABRIDE COMPLEX

The main exposure of Navado-Filabride rocks is an elongate structural culmination 125 km long and up to 35 km wide making up the major part of the Sierra Nevada and sierra de los Filabres. Nevado-Filabride rocks crop out in the cores of the Sierra Alhamilla and sierra Cabrera and in the sierra Almenara further east.

They comprise Nevado-Lubrin unit (graphite mica schist) and Tahal schist (light mica schist) (see Figure 3.2), Tourmaline, Quartz feldspar and mylonite, and Cacaes Marble, which their

age expected to be from Paleozoic to Permo-Triassic. There is evidence in the higher tectonic units of an early high P/low T metamorphism, reflected by locally preserved glaucophane schist and eclogite in the metabasic rocks. There is no evidence that the great thickness of green schist facies graphitic mica-schist and quartzite that makes up the core of the Sierra Nevada ever experienced the high-pressure metamorphism seen in the higher Nevado-Filabride units [14], but it was recognized that the lack of evidence for high pressure could be due to the rock composition. These are rocks currently distinguished as the Veleta Complex, whilst the higher Nevado-Filabride units are grouped in to the Mulhacen complex. The Mulhacen Complex has a structural thickness of several kilometres in the eastern Sierra de los Filabres but thins progressively westward [22], and over the whole western Sierra Nevada it is entirely encompassed within the mylonite zone, a few hundred meters thick, that marks the upper boundary of the Nevado-Filabride Complex as a whole. At high levels in the complex the structure is dominated by a strong sub horizontal foliation, commonly associated with isoclinal folds, and a stretching lineation that is warped around the regional culminations.

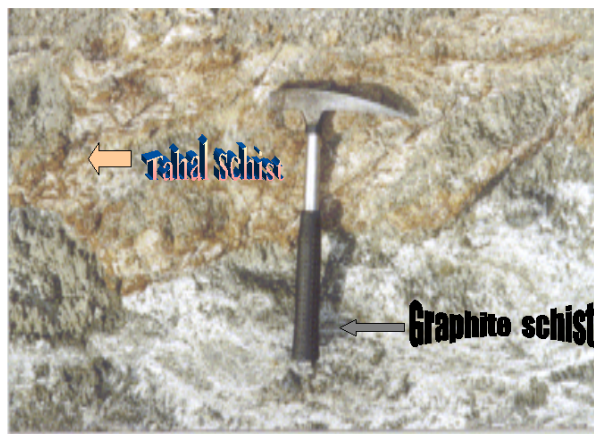


Figure 3.2: Graphite mica schist (light-dark) and Tahal schist (light-brown) (GRMEG, 2002).

3.3 ALPUJARRIDE COMPLEX

The Alpujarride complex includes Paleozoic rocks identical to those of the Nevado-Filabride Complex, Permo-Triassic aluminous phyllite (multicoloured phyllite and psammite) and quartzite, and a thick sequence of Middle to Late Triassic dolomitized platform carbonates (meta carbonates), which locally enclose mafic intrusives of unknown age. No post-Triassic rocks have been found. Much of the Alpujarride complex only shows lower green schist facies metamorphism, but occurrences of sodic amphibole and carpholite suggest that ambient pressures during this low-grade event may have reached 7 Kbar, corresponding to a moderately high PT ratio. In the Sierra Alhamilla, identify the contact between low green schist facies Permo-Triassic rocks above and amphibolite facies Paleozoic rocks below as an extensional fault [49]. In the Sierra de los Estancias, there is a transition from ductile extension associated with a regional flat-lying foliation, ductile shear bands indicating NE directed shear and a strong NE to ENE trending stretching lineation, to brittle north to NE directed normal faulting. This deformation was accompanied by high T, low P metamorphism and

was associated with the extensional contact between the Alpujarride and Malaguide Complexes.

3.4 MALAGUIDE COMPLEX

Exposures of the Malaguide complex are largely limited to the western Betics north of Malaga and to a thin strip along the internal-external zone boundary. It comprises a well-differentiated sequence of Palaeozoic clastic and carbonate rocks, Permo-Triassic red-beds, Middle to Late Triassic carbonate rocks and evaporates

3.5 SEDIMENTARY SUCCESSION

The following formations have been distinguished in the study area and their age ranges from Serravallian to Plio-Pleistocene and they are:

- Serravallian-Tortonian-Messinian Chozas Formation: Shows a high rate of subsidence.

Contemporaneous synsedimentary deformations (e.g. slumps and slide) as well as the random occurrences of megabeds in late Tortonian to early Messinian strata strongly suggest tectonic activity [37]. The Chozas Formation unconformably overlies the metamorphic rocks of the basin floor. The chozas formation is presented in Figure 3.3.



Figure 3.3: Turbiditic sandstone and marl overlain unconformably by conglomerate (Chozas Formation).

- Early Messinian Turre Formation: Shows rapid basement rise for this time of period. There is no folding phase in the Tabernas basin where folding and emergence of the Chozas strata occurred at the Tortonian-Messinian boundary. Uplift along NW-SE trending faults of the area East of road C-3326 occurred just before the advent of an evaporitic phase (Yesares Formation). This uplift is indicated by the presence of conglomerates and slump deposits in an area parallel to the faults and below the gypsum deposits and by the areal distribution of gypsum deposits. The Turre formation conformably covers the chozas Formation. Limestone reefs (M1) and conglomerates (M2) occur at the northern margin of the Tabernas basin where as mudstone laminites (M3) were deposited in the centre of the basin [38].

- Messinian Yesares Formation: The geohistory indicates continued basement rise during the Messinian. The Yesares Formation conformably overlies the marine mudstones (M3) of the Turre Formation. Reef-blocks in a slumped conglomeratic horizon 10 m below the gypsum deposits of the Yesares formation indicate the reef growth had taken place before the evaporitic phase.
- Early pliocene Abrioja Formation: The Tabernas Basin experienced subsidence and subsequent uplift in the early Pliocene. At the end of the Messinian, folding of Neogene deposits occurred parallel to the anticlinorium of the emerging Sierra Alhamilla. The Abrioja Formation overlies the Chozas, Turre and Yesares Formations erosively and unconformably [38].
- Plio-Pleistocene Gador Formation: Continued basement rise in the Plio-Pleistocene resulted in continental deposits that were contemporaneous with shallow marine deposits of the Abrioja Formation in the Rioja corridor and Almeria basin. The Gador Formation interfingers and later overlies the Abrioja formation [38].

3.6 QUATERNARY DEPOSITS

The Plio-Pleistocene sediments in the Tabernas basin experienced gentle folding along SW-NE directed axis. Two conspicuous levels of river terraces presumably of late quaternary age post-date the folding phase and are therefore separated from the Gador Formation. General geological map of the study area is presented in Figure 3.4.

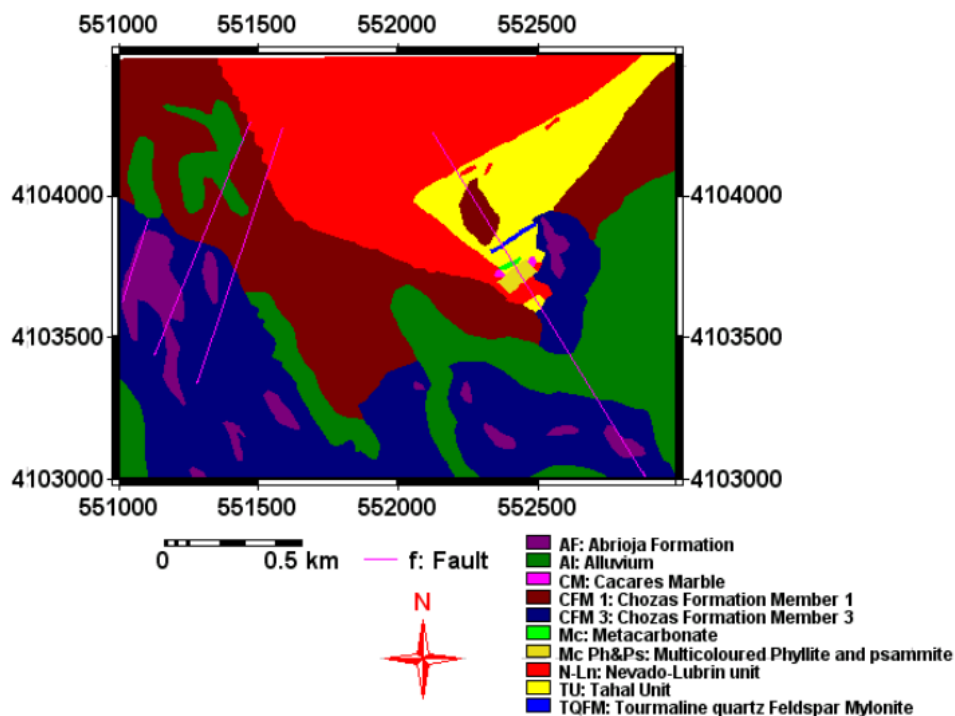


Figure 3.4: Geological map of study area (GRMEG, 2002).

3.7 GEOLOGY AND ENVIRONMENT

The Tabernas area is a place where the geological setting has played a great role in controlling the environmental conditions. The topographic features that resulted from different geological processes and lithology are the main controlling agents of the present environment. The two anticlinoriums, the Sierra Alhamilla and the Sierra de los Filabres, that run parallel almost in East-West direction, are controlling the climatic behaviour of the basin. The wind direction records of the solar plant near the town of Tabernas indicate a dominantly E-W direction, suggesting the strong influence of the two mountain ridges [13].

The salinity crisis of the geologic past, which happened during Late Miocene, resulted in one of the great events that shaped the current environment [21]. The contemporary salinity problem was initiated there.

The hogbacks and cuestas of the inclined beds of the soft marl, clay and sand beds have facilitated the severe erosion and the poor soil development condition. These and the extreme climatic nature have left the southwestern part of the study area as badland [3].

The dynamic tectonic activity that took place in the past and which is still active has complicated the environmental situations [32] [63]. Land-instability, rock fall and debris flow, are other environmental problems of the area that can mostly be attributed to the geological processes. The edge of the upper limb of the fold nappe of the Sierra Alhamilla has provided material for ancient landslides on which the village of Turrias, visible at the foot of Carro Munito, is built. Incipient surface movement of Carro Munito is indicated by open cracks up to 200 m deep. The underlying impermeable phyllite with its sub horizontal foliation presumably acts as a lubricant beneath the carbonates and allows creeping down the topographical slope [63]. The sandy and conglomeratic mega beds that form weathering resistant beds in the Neogene sedimentary sequence occur as a rock fall. The fall of mega beds in the Tabernas basin may be due to seismic enhancement of slope instability (*ibid*). The steep slopes and the nature of the rocks in association with the triggering forces of tectonism have created landslides in the geologic past. Even in the geologic past the slope instability feeding the turbidite fan complex may have been enhanced by further uplift of the Sierra de los Filabres during the Serrvillian-Tortonian period (*ibid*).

Apart from the above-mentioned visible geologic features, the subsurface hydrologic system is one of the main influenced zones by the geological setting. The lithologic and structural characteristic of the recharge and discharge zone directly and strongly influences the subsurface hydrologic system. The nature of aquifers, the availability, distribution and quality of ground water mainly depend on the geology. In this aspect the dominant aquifers of Desert of Tabernas, the sub-marine sediments, have salt bearing horizons, which make them potential sources of salinity to the soil as a result of capillary rise with intensified irrigation. The hydrologic system in the quaternary sediments is easy to be polluted by any percolating pollutants.

Chapter 4

MATERIAL, RESEARCH METHODS AND TECHNIQUES

4.1 INTRODUCTION

The use of remote sensing techniques to study soil erosion processes in the Mediterranean type of environments has been extensively applied in various projects during the past decade (MEDALUS, DEMON, ELANEM). In this chapter the more relevant characteristics of the remotely sensed data used to estimate the surface cover factor from NDVI of the study area is discussed. The techniques applied to process raw data, such as georeferencing; resampling and creation of submap from input image will be discussed.

4.2 MATERIALS

The following materials and equipments were used for research implementation.

- **Maps, images and photos for interpretation.**
 - Topographic map at scale 1:10,000(hard and soft copy).
 - DEM, to calculate slope factors (LS), and also to determine the erosion flow direction.
 - Landsat TM with bands of 1 to 7 (Path/Track: 199; Row/Frame: 34; Sensor Mode: Multi Spectral; Sensor: TM; Platform: LANDSAT 1/5; and Date: 1984-08-20)
 - Digital orthophoto at scale of 1:10,000.
 - Aerial photograph at scale 1:20,000
- **Softwares for image and data processing:**
 - Erdas, Arc View GIS version 3.3
 - Integrated Land and Water Information System (ILWIS) 3.1
 - ILWIS 3.0 RUSLE (Revised Universal Soil Loss Equation) Topographic Factor (LS) interface
- **Software for Documentation and Presentation:**
 - MS Word, LaTeX, WinEdt, MS Power point, MS Photo editor, PDF and MS paint
- **Ancillary Data:**
 - Publications, different reports and records on geology, soil erosion, geomorphology, soil data, climate (Rainfall data, 1968-1990) and etc.

4.3 METHODOLOGY

Traditional approaches in the assessment of soil erosion usually involve the production of maps showing the extent and intensity of morpho-dynamic processes, such as sheet or gully erosion, analysis of vegetation characteristics, land cover and land use distribution. Commonly, they are based on aerial photograph usage and the results are subjective and some times can over estimate the extent of degradation (erosion) [48]. Spectral contrast between bare soil and vegetation or between different levels of vegetation cover at the scale of whole landscapes can be used to develop supportive measures of soil erosion [42] [48]. To accomplish the formulated objectives, the first step was a literature review on the main aspects of soil erosion and the use of remotely sensed data for this study. Then, being the surrogate data for this research, an extensive literature review and data collection through internet was made so as to obtain the previous studies and works carried out in the Tabernas area.

4.4 DATA ANALYSIS, IMAGE PROCESSING AND INTERPRETATION OF REMOTE SENSING AND GIS DATA

4.4.1 DATA ANALYSIS

Prior to image interpretation all data related to the area of study were analyzed and corresponding image data were identified and separated from the rest of images for image interpretation. By and large the revising of the literature review was the core of this research work, as it totally helped the research work.

4.4.2 IMAGE DATA HANDLING

The aim of image interpretation is to evaluate the advantages of the visual and digital interpretation of satellite imagery and the contributions of the techniques of improvement of remotely sensed data applied to soil erosion in the study area (northwest of Tabernas). There are two ways to approach image interpretation [6]: One was by means of visual and qualitatively oriented interpretation of analogue images. The other involves the digital and quantitatively oriented interpretation of digital images. In visual interpretation, an interpreter evaluates several image characteristics (tone, texture, size, pattern, association) in order to identify and deduce the significance of the components of the image. Digital analysis, considered a less subjective method concerns numerical quantities, defined decision criteria or the application of logical operators.

DIGITAL IMAGE PROCESSING

Digital image processing involves:

- Geometric correction;
- Density slicing; and
- Re-sampling.

Geometric correction

When an image (raster map) is created, either by a satellite, airborne scanner or by an office scanner, the image is stored in row and column geometry in raster format and there is no relationship between the rows/columns and real world coordinates (UTM, geographic

coordinates or any other reference map projection). In a process called geo-referencing the relation between row and column numbers and real world coordinates are established.

In this study, geo-referencing the remotely sensed datasets include:

- Geo-reference corners: Specifying the coordinates of the lower left (as xmin, ymin) and upper right corner (as xmax, ymax) of the raster image and the actual pixel size. A geo-reference corners are always north-oriented.
- Geo-reference tiepoints: Specifying reference points in an image so that specific row/column numbers obtain a correct X, Y coordinate. All other rows and columns then obtain an X, Y coordinate by an affine, second order or projective transformation as specified by geo-reference tiepoints. A geo-reference tiepoints can be used to add coordinates to a satellite image or to a scanned photograph and when there is no DTM.

And therefore, as it is mentioned above the image without coordinate first geo-referenced by approach of *tiepoints* using the other image that already geo-referenced. During geo-referencing the image the sigma value was 0.287.

Re-sampling

After geo-referencing an image, the image will have coordinates for each pixel, but its geometry is not corrected for geometric distortions and not adapted to a master map or image. In order to create a distortion free adapted image, the transformation defined above is executed.

This results in a new image in which the pixels are arranged in the geometry of the master image or map and the resolution is equal to the resolution of the master image. The latter was then used for classification of Normalized Difference Vegetation Index (NDVI).

Density slicing

Density slicing is a technique, whereby the DNs distributed along the horizontal axis of an image histogram, are divided into a series of user-specified intervals or slices. The number of slices and the boundaries between the slices depend on the different land covers in the area. All the DNs falling within a given interval in the input image are then displayed using a single class name in the output map. The approach of density slicing was used in NDVI classification to remove (subtract) the values of water from bareland areas.

Submap

The submap operation allows the image processor to specify a rectangular part of a raster map and copy it into a new raster map. The image processor can specify corners either in rows and column numbers or in XY coordinates. For creation of submap a raster map with any type of domain can be used as input and the output map uses the same domain as the input map. Then, the operation automatically creates a new geo-reference for the output map. Similarly during this research the corners were specified in the UTM zone that have the XY coordinate values of min X: 551000, min Y: 4103000; and max X: 553000, max Y: 4104500.

4.4.3 SPATIAL DATA ANALYSIS

Filtering

Filtering is a process in which each pixel value in raster map is replaced with a new value, provided that a condition or a set of conditions is satisfied. The new value is obtained by

applying a certain function to each input pixel and its neighbours. Of the many types of filters used in ILWIS the Majority filter was selected during the NDVI classification.

GIS applications

GIS operations were applied to data integration with the objective of monitoring the erosion process. The digital maps corresponding to year 1984 (Landsat TM 7203 or tm7203) was applied for NDVI processing and NDVI classification.

4.4.4 COLOUR COMPOSITE

False Colour Composites as seen in Figure 4.1 was created for the study area using Landsat TM bands 4, 3 and 2 (in RGB order) and this image was acquired on 20/08/1984. In this combination, vegetation appears Reddish, water Bluish and bare soil (bareland) in shades of DimGray and Gray. The purpose of visualization of multi band images (False Colour Composites) was to identify, extrapolate and correlate the spectral information with that derived from the NDVI.

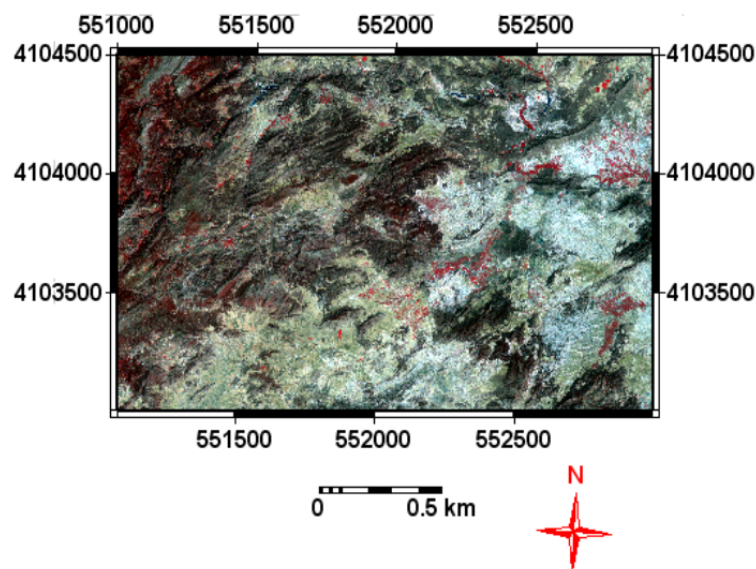


Figure 4.1: False colour composites (vegetation: Reddish; bareland: DimGray and Grey and water: Bluish).

4.4.5 NORMALIZED DIFFERENCE VEGETATION INDEX (NDVI)

Mathematical combinations of the TM 3 visible band (0.63 to 0.69m) and TM 4 near infrared band (0.76 to 0.9m) have been found to be sensitive indicators of the presence and condition of green vegetation because vegetated areas have a relatively high reflection in near-infrared band. The NDVI was created using the arithmetic combination of the original spectral bands: $NDVI = (TM\ 4 - TM\ 3) / (TM\ 4 + TM\ 3)$. In the NDVI image which have values ranging from -0.73 to 1.0; water and cloud show negative values -0.73 to 0 (the fact that they have higher reflectance in red (visible) than in near infrared wavelength). Rock and bare soil have values around zero (0 to 0.02) because they have similar reflectance values both in red (visible)

and near infrared wavelength. Vegetation has higher reflectance in near infrared than in red (visible) wavelength and as a result has positive values (0.02 to 1.0) with higher values associated with higher densities of green and healthy biomass stated [28]. But as it can be seen in the NDVI map most areas have values of water, which is practical impossible in real nature of the study area and it might be due to the fact that the image was acquired on rainy and/or cloudy day. Therefore to remove the effect of cloud and/or shadow from bare soils (bareland) the approach like density slicing was applied. This means that in the NDVI map most areas have the values of water or values of 0 to -0.73, but the actual water areas has the values of -0.41 to -0.73, and the rest areas that covered by water values (-0.41 to 0) refer to the areas of bare soils. These values were approved by reading the areas that occupied by water and the areas of bare soils (bare land) in FCC and also in NDVI (water appears in Blue). The Normalized Difference Vegetation Index (NDVI) is a measure of the amount of green cover at the earth surface. The quantification of NDVI is relative and not absolute, and therefore it provides a measure of which areas of vegetation are more vigorous than others [28]. The map that shows the NDVI values is presented in Figure 4.2.

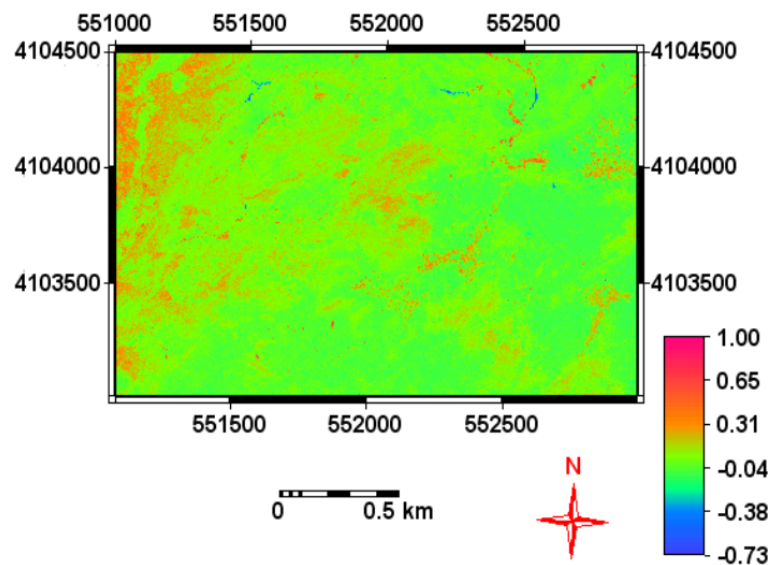


Figure 4.2: Map of NDVI.

- **Classification of Normalized Difference Vegetation Index (NDVI)**

In the classification of the different land cover classes using NDVI the availability of field collected data is important for verification. In this study however, since there was no field data to validate the result and do proper classification of the imagery, the NDVI result was used in its broadest sense to differentiate 3 major land cover classes namely; water, vegetation and bare soils and the classes are presented in Figure 4.3.

The resulting image discriminates in vegetated areas with NDVI values of 0.02 to 1.00; bare soil or bare land with NDVI values of -0.41 (but -ve value removed by density slicing) to 0.02; and areas covered by water showing NDVI values of -0.41 to -0.73 refer Figure 4.2.

As it can be seen in NDVI classified map in Figure 4.3 the rocks and bare soil appear in *Red*; vegetation appear in *LawnGreen* and water in *Blue*. In arid and semi-arid environments the study of green vegetation from satellite multi-spectral observation is hampered by the influence and variability of soil back ground, where vegetation cover is sparse and the reflectance

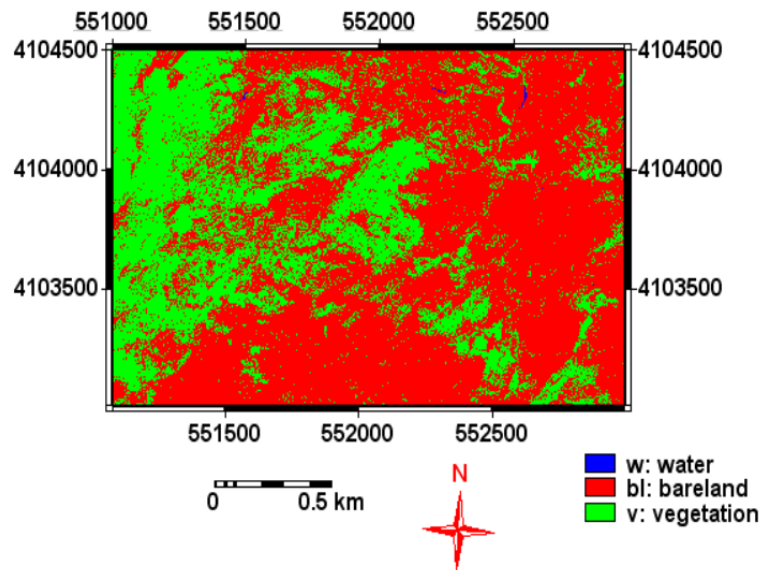


Figure 4.3: Map of NDVI Classified.

of the underlying soil becomes a significant factor [28].

4.5 CONCLUSIONS

The contribution of remote sensing to map the spatial distribution of the land cover focusing on the identification of erosion related classes has been "*partially*" illustrated in this chapter. Different approaches, methods and techniques were tested in the study area (northwest of Tabernas) to explore their potentials and limitations to map the land cover associated with soil erosion features.

- This chapter has dealt with the study of satellite imagery (Landsat TM) in respect of geo-referencing, re-sampling, density slicing and creation of submap, and basically colour composite and NDVI were generated prior to the image classification.
- Image enhancement procedures are applied to image data in order to more effectively display or record the data for subsequent visual interpretation.

During classification of NDVI most of the areas have values of water, which is practically impossible with the real nature of the study area and it was probably due to the fact that the image was acquired on the rainy day and the areas of bare soils have values of water, and this effect of cloud and/or shadow was removed by density slicing.

In this study, it has observed that once more the importance of integrated field observations with remotely sensed data as an approach to produce thematic information in the earth sciences.

To sum up with, the Normalized Difference vegetation index (NDVI) is a measure of the amount of green cover at the earth surface and the quantification of NDVI is relative and not absolute.

Chapter 5

SOIL EROSION (SOIL LOSS) ASSESSMENT

5.1 INTRODUCTION

Soil erosion is one form of soil degradation along with soil compaction, low organic matter, loss of soil structure, poor internal drainage, salinisation and soil acidity problems.

Soil erosion is a naturally occurring process on all land and it is a normal geologic process associated with the hydrologic cycle. The agents of soil erosion are *WATER and WIND*, each contributing a significant amount of soil loss each year. This study of soil erosion is concerned with soil erosion by *water (rainfall)*. In humid climates where vegetation is dense, soil erosion by water is normally very low and the characteristic soil profiles are maintained as erosion proceeds. In arid climates, like Tabernas, especially where a rock is of a weak and highly impermeable nature, normal erosion is rapid and furnishes vast quantities of sediment to streams [55].

The erosion of soil from land areas can significantly damage the terrestrial habitat and can also have serious environmental impacts. Soil erosion may be a slow process that continues relatively unnoticed, or it may occur at an alarming rate causing serious loss of topsoil. The loss of soil from farmland may be reflected in reduced crop production potential, lower surface water quality and damaged drainage networks.

The following are the erosion processes and types:

- Soil detachment caused by rainfall and overland flow;
- Rill erosion and transport;
- Gully erosion;
- Channel degradation and bank erosion;
- Surface gravity erosion, and wind erosion.

Gully and Sheet erosions are highly pronounced erosion types in the study area.

5.1.1 SHEET EROSION

It is a type of **surficial** process that is developed specifically when the soil loses its vegetation cover and is exposed to the atmospheric agents such as raindrops. Raindrops striking exposed soil detach the soil particles and splash them into the air and into shallow overland flows. Raindrops striking these shallow flows enhance the flows turbulence and help

to transport more of the detached sediment to a nearby rill or flow concentration.

when surface runoff is initiated it may be in *sheet* form or where the irregularities of the surface demand it, the form of filaments of flow in a complex braided pattern [10]. Sheet erosion is the uniform removal of soil in thin layers by the forces of raindrops and overland flow. It can be a very effective erosive process because it can cover large areas of sloping land and go unnoticed for quite some time. It consists in the detachment of individual soil particles and further accumulation in a place different of its origin but generally close to it.

5.1.2 GULLY EROSION

Gullies have been defined from different perspectives, e.g. agricultural and landscape. From a landscape perspective, gullies are defined as steep-sided eroding watercourses that are subject to ephemeral flash floods during rainstorms [44] [31] [19]. It is deep enough to interfere with and not to be obliterated by normal tillage operations (soil science society of America Journal, 1987). Thus, gully erosion is often an advanced stage of rill erosion, much as rill erosion is often an advanced stage of interrill erosion. The rate of gully erosion depends on the runoff producing characteristics of a slope or landform, the drainage area, soil characteristics (resistance of the soil to erosion), the alignment, size and shape of the gully, the slope in the channel and the vegetation. Gully erosion mostly occurs when the subsoil consists of loose material [25].

In the development of a gully, many processes may take place either simultaneously or during different periods of its growth. The most important processes are: water erosion at the gully head, channel erosion caused by water flowing through the gully and slides or mass movement of soil in the gully. The effect of Gully erosion in Uplifted and faulted Miocene marls (Chozas Formation) within and near to the study area is presented in Figure 5.1.



Figure 5.1: Uplifted and faulted Miocene marls (Chozas Formation) are being eroded by surface processes, leading to the formation of gully and valleys (Mitchell, 1995).

Erosion also occurs on a larger scale episodically due to channel bank and hill slope failures, *land sliding*, forest fires and debris flows. Land use practices such as logging and clearing, grazing, *road construction*, agriculture and urbanization activities also affect sediment production and delivery from a watershed. A distinguishing between natural or geological soil erosion and soil erosion accelerated by human activity is an important point in the area of study as the human activities facilitate highly the soil erosion.

5.2 CLASSIFICATION OF PHYSIOGRAPHIC ZONES FOR SEDIMENT GENERATION AND DEPOSITION

It is instructive to divide soil erosion into major zones or provinces where different sets of physical processes interact to characterize sedimentation processes.

There are three physiographic zones suggested in literature:

1. Production zone or sediment source area;
2. Transfer zone; and
3. Deposition zone or sediment sink area.

On a geologic time scale, the surface of the earth is transformed by sediment production (erosion) in the upper part of the watershed; transportation of sediments in a fluvial system; and deposition of sediment carried by water is likely any where that the velocity of running water is reduced at the mouth of gullies, at the base of slopes, along stream banks, on alluvial plains, in reservoirs, and at the mouth of streams and in the seas. In this research of specific study area (northwest of Tabernas), depending on altitude difference, three physiographic zones were derived from DEM of study area and the map of DEM of physiographic zones are presented in Figure 5.2 5.3.

It has to be understood that when said production zone, it does not mean that areas of high erosion risk, but the areas of high altitude and it may be on top of mountains or hills with flat areas and sheet erosion and without deposition taking place over there. According to this physiographic classification the production zone ranges in altitude (meter) from 506-595; the transfer zone from 430-506; and the deposition zone from 417-430 a.m.s.l.

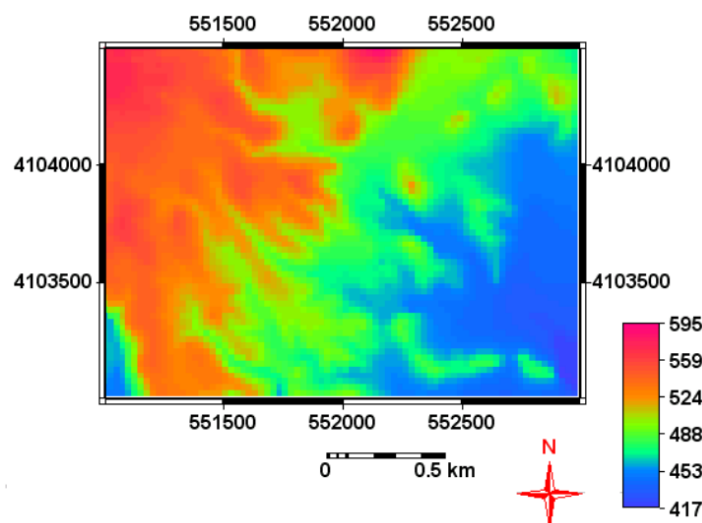


Figure 5.2: Map of DEM of study area.

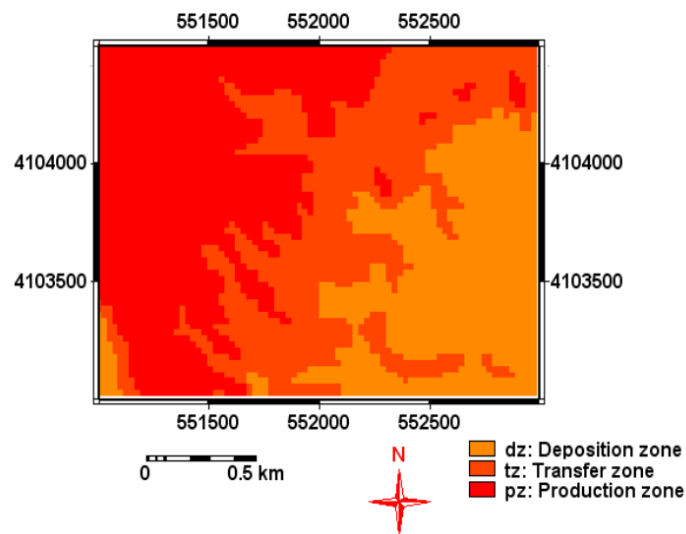


Figure 5.3: Map of physiographic zones.

5.3 PREDICTION OF SOIL EROSION BY WATER USING RUSLE

During this research the estimation of soil erosion by water was related to *natural or geological soil erosion* and it was because of that in the study area, the erosion risk is high in the areas of non-agriculture than the areas of agriculture. And the erosion risk is highly pronounced in the areas of rugged topography and that of not suitable for agricultural activities. Due to the fact that most of the agriculture areas are located in the flat areas or at the areas of sediment deposition, and as erosion risk in those area is too low, there was no need to estimate soil erosion in such areas (agricultural areas).

This research work of estimation of soil loss by water was carried out by using Revised Universal Soil Loss Equation (RUSLE).

RUSLE is an "upgrade" of the Universal Soil Loss Equation (USLE) initiated in 1985. RUSLE is a computerized model and it is possible to evaluate conditions not possible with the Universal Soil Loss Equation (USLE). RUSLE has the same formula as USLE, but has several improvements in determining factors. These include some new and revised isoerodent maps; a time-varying approach for soil erodibility factor; a subfactor approach for evaluating the cover-management factor; a new equation to reflect slope length and steepness; and new conservation-practice values [40]. RUSLE can be used on crop lands, pasture lands, land fills, mining sites, reclaimed sites, military training lands, parks, land deposal of waste, disturbed forest lands, construction sites, and other areas where surface overland flow occurs because rainfall is greater than infiltration (refers to this research area).

The Revised Universal Soil Loss Equation (RUSLE) [40] and handout provided by Mannaerts (2002) were used as a modelling instrument and a main reference to estimate soil erosion in this research work.

- In this research of estimation of soil erosion by water 5 major factors were considered:
 1. Climate (rainfall).
 2. Soil and geologic parent material.

3. Topography and/or relief.
 4. Land cover (Vegetation).
 5. Human impacts/conservation practice.
- The estimation of soil erosion by water using RUSLE equation is defined as follows:
 - $A = K \cdot R \cdot (LS) \cdot CP$
 - A = Computed soil loss per unit area (tons/ha/yr) or (ton/acre/yr);
 - K = Dimensional Soil Erodibility Factor(tons/ha/yr)/(MJ/ha*mm/hr);
 - R = Dimensional Rainfall-Runoff Erosivity Factor (Index) (MJ/ha*mm/hr);
 - LS = Slope Factors (unit less);
 - C = Cropping Management Factor (unit less); and
 - P = Conservation Practice Factor (unit less).

The general flow chart of RUSLE application is presented in Figure 5.4.

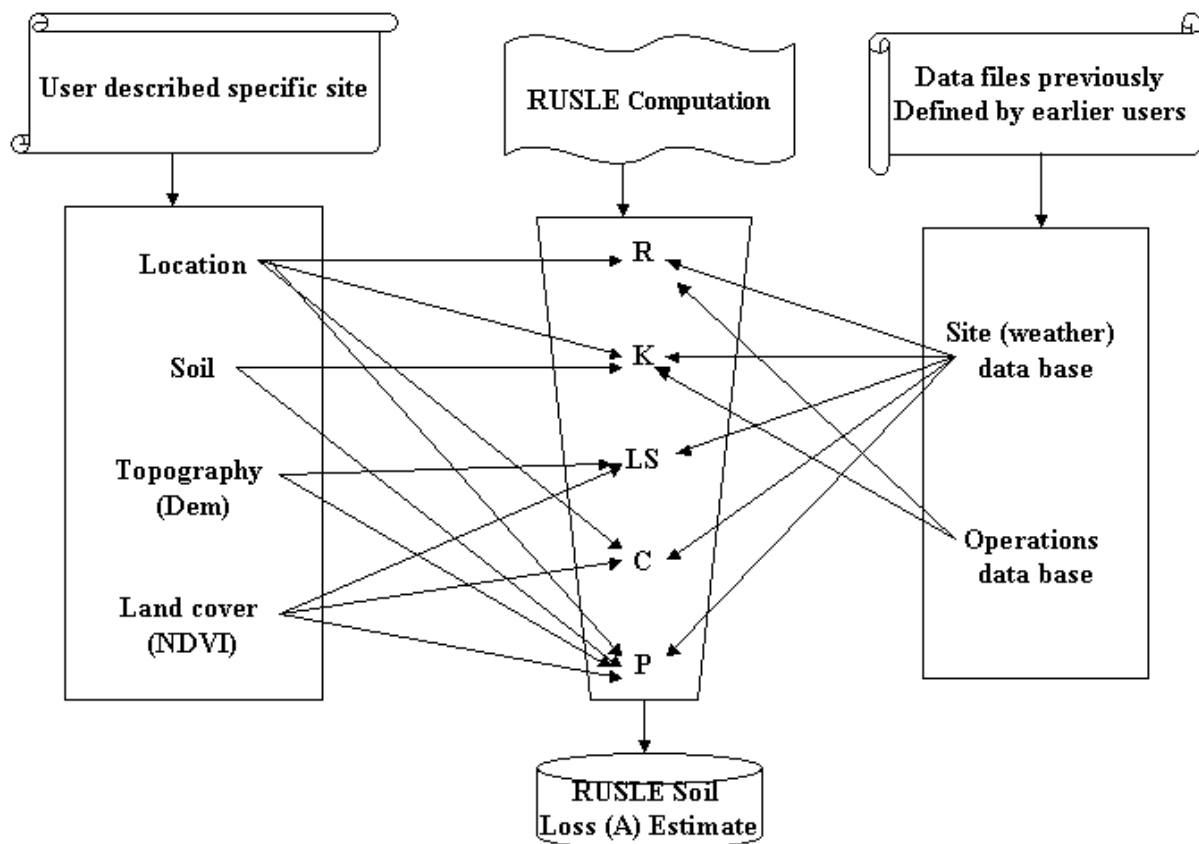


Figure 5.4: General Flow Chart of RUSLE.

5.3.1 RAINFALL-RUNOFF EROSIVITY FACTOR (R)

The rainfall-runoff erosivity factor (R) refers to climate (rainfall) factor. The agents for the erosion are raindrops and flowing water. Raindrop, rain splash or splash erosion is the process of erosion on barren soil surfaces. The moisture content existing before the rainfall affects the overland flow production. The overland flow volume is much higher when the soil is saturated, or nearly to so, at the time when the rain starts to fall Nill (1996). This overland flow involves the dislodgement and movement of soil particles under the impact of falling raindrops. Runoff erosion largely concerns the transportation of loose material (much of it often prepared by raindrop erosion) by turbulent water flowing as unconcentrated flow in sheets, or as concentrated flow in rills or gullies, although some detachment of particles also occurs in runoff erosion [10].

- The rainfall erosivity, in addition to detaching primary particles, energy from rainfall on unprotected soil surface enhance erosion by:
 - Breaking down aggregated particles making the material easier to transport;
 - Promoting surface seals that reduce infiltration and therefore increase runoff;
 - Moving particles down slope or directly into rills by splash; and
 - Promoting turbulence in runoff that increases transport capacity.

R is the average annual summation (EI) values in a normal year's rain. The erosion-index (EI) is a measure of the erosion force of specific rainfall. When other factors are constant, storm losses from rainfall are directly proportional to the product of the total kinetic energy of the storm (E) times its maximum 30-minute intensity (I). Storms less than 0.5 inches (12.7mm) are not included in the erosivity computations because these storms generally add little to the total R-value (www.iwr.msu.edu). R is an indication of the two most important characteristics of a storm determining its erosivity: amount of rainfall and peak intensity sustained over and extended period.

The causes and effects of erosion in the province of Almeria, one of the most severely eroded Spanish provinces, among the other factors is the climatic situation [51]. He reported for the meteorological station of Topares a rainfall intensity of 200 mm in 60 minutes for an assigned return period of 50 years. Studies involving rainfall simulation shows that some rainfall detachment parameters can be drop size distribution, fall velocities and mass at impact [30].

The rainfall in arid and semi-arid areas are intense and has a short period of duration and have the value of rainfall erosivity factor (R) higher than the rainfall in highland and tropical areas. Similarly, the Tabernas Desert located in semi-arid areas has intense and short duration rainfall and has high rainfall erosivity factor (R). As it is mentioned in chapter two the Tabernas area has a mean annual precipitation of 218 mm and the maximum recorded rain intensity at the on-site meteorological station during the year 1992-93 was 85.2 mm/hr during 5.7 minutes, which indicates that the intensive rainfall for short period of times.

Rainfall Intensity and Runoff

Both rainfall and runoff factors must be considered in assessing a water erosion problem. The impact of raindrops on the soil surface can break down soil aggregates and disperse

the aggregate material. Soil movement by rainfall (raindrop splash) is usually greatest and most noticeable during short duration, high intensity thunderstorms. Although the erosion caused by long lasting and less intense storms is not as spectacular or noticeable as that produced during thunderstorms, the amount of soil loss can be significant, especially when compounded over time. Runoff can occur whenever there is excess water on a slope that cannot be absorbed into the soil or trapped on the surface. The amount of runoff can be increased if infiltration is reduced due to soil compaction, crusting or freezing.

Rainfall Kinetic Energy

Hudson (1971) added an "effective erosion" threshold that rainfalls greater than 25 mm/hr are important in causing erosion.

But very dependent upon:

- Type of rainfall (storm/depression);
- Antecedent soil moisture;
- Total rainfall amount; and
- Season.

For estimation of kinetic energy a new recently proposed formula [5], which applies for all intensities is given below.

- $E(SI) = 0.29 \cdot (1 - 0.72 \cdot \exp(-0.05(I)))$
- E = kinetic energy of 1 mm of rain of intensity, I in (MJ/ha.mm) and I in (mm/hr)

But the computation of kinetic energy was not carried out for the reasons that there was no data that include the single storm precipitation and/or 30 minutes or hourly rainfall (precipitation).

Estimation of Annual Rainfall-Runoff Erosivity Factor (R)

The estimation of annual rainfall erosivity was done using the regional (statistical) regression indices (e.g. modified Fournier equation). The rainfall database was obtained from the Spanish Meteorological Office that includes the rainfall data from 1968-1990.

The formula used for the study area to compute the annual rainfall erosivity factor (R) is $R = 5.44 \cdot (\sum (P_i^2 / P_{an})) - 1.52$

Where,

- R, annual erosivity;
- P_i , monthly rainfall depth; and
- P_{an} , annual rainfall.

The estimated annual rainfall erosivity is presented in Table 5.1.

Month	R 1984	
	Rainfall (mm)	Pi^2/P_{an}
Juan	27	3.591
February	18	1.596
March	20	1.970
April	26	3.33
May	12	0.709
June	8	0.315
July	1	0.005
August	1	0.005
September	11	0.596
October	28	3.86
November	31	4.734
December	20	1.970
Total	203	22.68
Annual Erosivity(R)		121.88

Table 5.1: Estimated Annual Rainfall Erosivity Factor (R) (MJ/ha.mm/hr.)

5.3.2 SOIL ERODIBILTY FACTOR (K)

The soil erodibility factor (K) refers to soil and geologic parent material factor. Soil erodibility factor K represents both susceptibility of soil to erosion and the rate of runoff. Erodibility of soil by erosion or running water related with percentage organic mater, particle size, sodium adsorption ratio (SAR), dissolved solids concentration in pore water and temperature [46] [52].

Generally, soils with faster infiltration rates (permeable), higher levels of organic matter and improved soil structure have a greater resistance to erosion. Soils high in clay have low K values, because they are resistant to detachment. Coarse textured soils, such as sandy soils also have low K values, because of low runoff even though these soils are easily detachable. Medium textured soils, such as silty loam soils, have a moderate K values, because they are moderately susceptible to detachment and they produce moderate runoff. Soils having high silt content are most erodible of all soils. They cause a decrease in infiltration and can also be cause for a formation of a soil crust, which tends to "seal" the surface and produce high rates of runoff. Values of K for these soils tend to be greater than 0.4. Organic matter reduces erodibility because it reduces the susceptibility of the soil to detachment, and it increases infiltration, which reduce runoff. The soil of study area (Tabernas) is developed from unconsolidated poorly to moderately sorted matrix supported alluvial deposits, calcarous, mica materials and quartzites, poorly sorted conglomerates, turbiditic sand and marl; and hence according to the soil particle diameter values they are categorized under moderate erodible soil.

The factors that can influence soil vulnerability to erosion include:

- Texture;
- Depth; and
- Surficial stoniness.

Soil texture classification is given in Table 5.2.

Fraction name	Size range (mm)
Clay	0-0.002
Silt	0.002-0.05
Very fine sand	0.05-0.1
Fine sand	0.1-0.2
Medium sand	0.2-0.5
Large sand	0.5-2.0

Table 5.2: Size limits of soil texture classification (world soil data set)

Depending upon the soil vulnerability to erosion each factor (texture, depth and surface stoniness) is divided into major/minor categories.

Referring to texture, the following soil categories will be considered:

- Highly erodible: sandy loam, loam, silty loam, silt;
- Moderately erodible: sandy clayey loam, clayey loam, silty clayey loam, loamy sand, sand; and
- Least erodible: sandy clay, clay, silty clay.

The triangle that shows the textural classes for soil erodibility is presented in Figure 5.5.

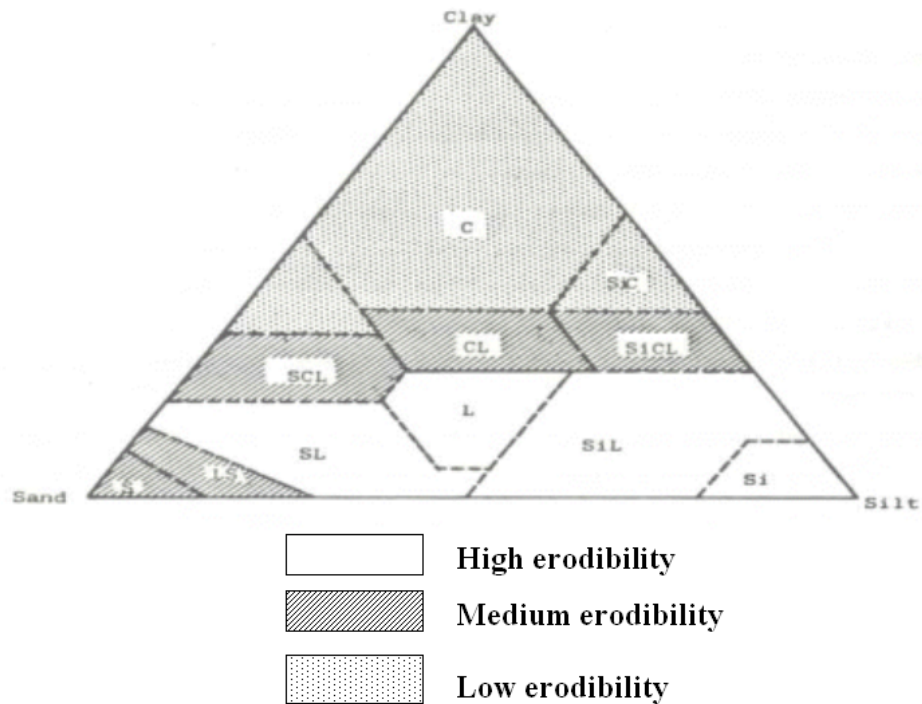


Figure 5.5: Textural classes for soil erodibility prediction.

The categories corresponding to soil depth include:

- Extremely vulnerable: soils whose thickness is less than 25 cm;
- Moderately vulnerable: soils whose thickness ranges from 25 to 75 cm;

- Least vulnerable: soil whose thicknesses is more than 75 cm.

The categories corresponding to surface stoniness include:

- Not predicted: soils lacking stones or with scarce stoniness; and
- Predicted: very stony soils.

It is known that the soil characteristics of the study area (northwest of Tabernas) are strongly controlled and influenced by the nature of the parent materials and the geologic forces prevailing in the area, and most of the soils developed from alluvial deposits of Nevado-Filabride complex (graphite mica schist and light mica schist) and Tabernas-Sorbas basin (marl). As their thickness is less than 25 cm they are categorized under soils of extremely vulnerable, and according to the category of surface stoniness they are categorized under the group of very stony soils. Similarly depending on *soil character* and *map unit* of the research area, the following erosion categories and related areas of deposition are defined as follows:

- Highly eroded areas: In Chozas Formation Member 3 (marl); and Multicoloured phyllite and psammite;
- Moderately eroded areas: In Chozas Formation Member 1 (poorly sorted clast supported conglomerate and breccia dominated by graphite boulders) ;
- Least eroded areas: In Nevada-Lubrin unit, Tahal unit, cacares marble, Abrioja Formation, Meta carbonate and Tourmaline quartz feldspar mylonite; and
- Deposition areas: In Alluvium. The map shows categories of soil vulnerability to erosion and deposition areas is presented in Figure 5.6

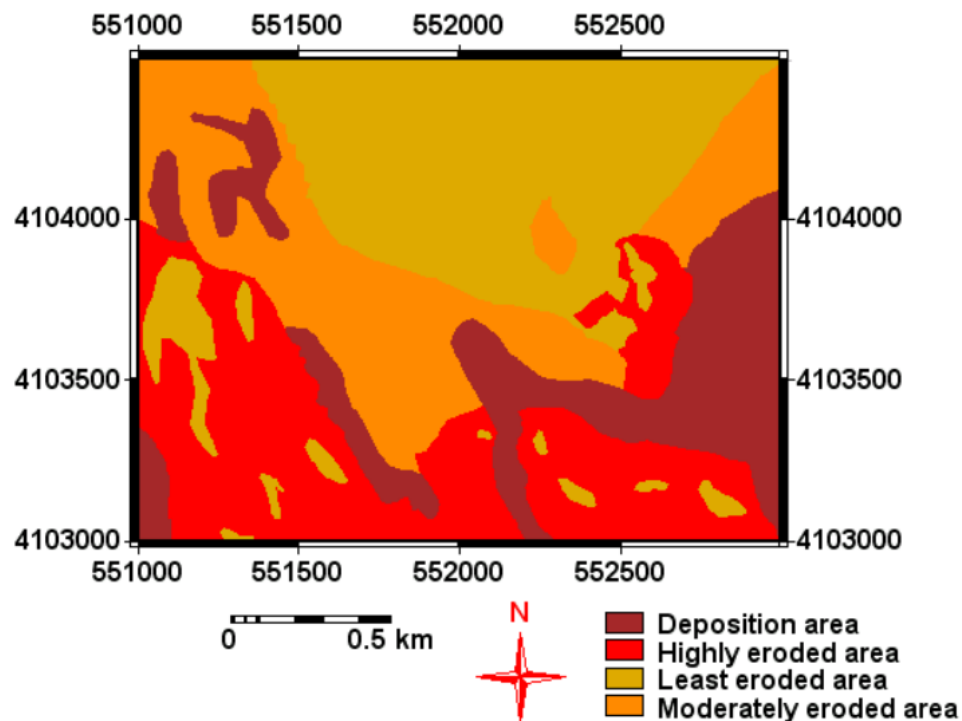


Figure 5.6: Map of categories of soil vulnerability to erosion and deposition areas.

Estimation of soil erodibility factor

Soil erodibility factor(K) is expressed in;
(ton/ha.hr)/(MJ/ha*mm/hr) or soil loss/rainfall erosivity.

There are two methods to estimate soil erodibility factor.

Method 1

The equation of the Wischmeier soil erodibility nomograph.

$$K=(1/7.594*[2.1*10^{-0.4} * (12 - OM)M^{1.14} + 3.25(s - 2) + 2.5(p - 3)]/100).$$

Where,

- K soil erodibility factor [$t.ha^{-1}.MJ^{-1}.ha.mm^{-1}.h$];
- OM, organic matter;
- S, code for soil structure;
- p, code for permeability; and
- M product of primary particle size fractions or (percent si+percent very fine sand (vfs))*(100-clay percent).

The soil data from past MSc thesis of Palacio (2002) [47] that includes percent organic matter has no coordinates to specify (locate) the sites where the samples were taken, and as a result it was not used as input in soil erodibility factor (K) to estimate soil loss (A). But as the data has percent organic matter and most of the RUSLE modelling for estimation of soil loss use this equation, it was taken to compare the values of soil erodibility factor (K) and annual soil loss (A) against the value of the mean geometric particle size (world soil data set) taken from soil data of MSc thesis (Tilahun, 2002) with coordinates. During estimation of soil erodibility factor (K), as the samples taken from different stations and reflect the entire soil textures of the study area the average soil erodibility factor (K) value was taken. The table that shows the estimated values by equation of the Wischmeier soil-erodibility nomograph is presented in Figure 5.7.

Sample station	Clay %	Silt %	Sand %	OM %	Structure	Permeability	K factor	Texture
JP-05	9.78	19	71.22	1.38	2	3	0.014	Sandy loam
JP-11	2	13.49	84.51	1.72	4	1	0.012	sand
JP-12	0.76	17.4	81.85	0.34	3	2	0.017	Loamy sand
JP-16	5.5	24.93	69.56	1.38	2	3	0.021	sandy loam
JP-18	1.01	17.95	81.03	0.52	3	2	0.017	loamy sand
JP-19	4.03	11.8	84.17	1.38	4	1	0.011	sand
Average	3.85	17.43	78.72	1.12	3	2	0.015	Loamy sand

Figure 5.7: Estimated soil erodibility factor (K) by the equation of Wischmeier soil-erodibility nomograph, and K in [ton/ha per MJ/ha*mm/yr].

Method 2

This method involves the mean geometric particle size (world soil data set) equation.

5.3. PREDICTION OF SOIL EROSION BY WATER USING RUSLE

$$K = (0.0034 + 0.0405 \cdot \exp(-1/2(\log(Dg) + 1.659/0.7101)^2)); \text{ and } Dg(mm) = \exp(0.01 * \sum(fi * \ln mi))$$

Where,

- K, soil erodibility factor $t.ha.h.ha^{-1}.MJ^{-1}.mm^{-1}$; Dg , mean geometric particle diameter (mm);
- f_i , primary particle size fraction (%); and
- m_i , arithmetic mean of the particle size limits of that size (mm).

The estimation of soil erodibility factor (K) using the equation of the mean geometric particle size (world data set) was done on the soil data obtained from (Tilahun, 2002) [36], which has coordinates but lacks organic matter, and it also lacks sand size (particle diameter) classes like percent very fine sand, percent fine sand, percent medium sand and percent large sand, and it only consists of the particle diameter of percentage of clay, silt and total sand. The soil samples were collected by Tilahun (2002) not for the purpose of soil loss estimation but in order to analyze the soil samples with respect of ion exchange for evaluation of salinity crisis in the areas. Hence, since there was no data on sand size (particle diameter) classes, the estimation of soil erodibility factor (K) was carried out by using the available % total sand, and also as only one sample with station number of 25 falls within the study area, and as this single value does not represent the soil texture of the entire study area to compute the soil erodibility factor (K) of the study area, the average of all samples was taken to compute soil erodibility factor (K). And similarly the average values was used to estimate annual soil loss (A) of the study area. The table shows the soil texture and average soil erodibility factor (K) value is presented in Figure 5.8.

Station no.	Clay %	silt %	Sand %	Log(Dg)	K factor	Soil texture
25	19.75	44.14	36.11	-1.401	0.041	Loam
27	31.36	1.56	67.08	-1.167	0.035	Sandy clay loam
40	58.79	38.86	2.35	-2.387	0.027	Clay
46	5.49	19.91	74.6	-0.705	0.020	Loamy sand
7	9.75	8.4	81.85	-0.672	0.019	Loamy sand
115	2.69	47.76	49.55	-0.987	0.029	Sandy loam
76	4.07	74.64	21.29	-1.369	0.041	Silty loam
114	32	44.24	23.77	-1.733	0.044	Clayey loam
63	6.85	14.07	79.08	-0.667	0.019	Loamy sand
69	22.94	65.17	11.898	-1.757	0.044	silty loam
58	37.73	47.17	14.61	-1.931	0.041	Silty clay
Average	21.04	36.902	42.017	-1.343	0.040	Loam

Figure 5.8: Estimated soil erodibility factor (K) by mean geometric particle size (world soil data set) method and K in [ton/ha per MJ/ha*mm/hr].

5.3.3 SLOPE LENGTH AND SLOPE STEEPNESS FACTORS (LS)

The slope factors (LS) refer to topographic and/or relief factor. In the computation of the LS factors, the topographic factors, L and S factor are usually considered together. The slope length factor L, computes the effect of slope length on erosion and the slope steepness factor S, computes the effect of slope steepness on erosion.

Longer slope lengths generate larger volumes of cumulative runoff and its velocity and depth. This will lead to scour erosion which would not occur on a shorter length of slope, or where the effective down-hill slope is reduced to the distance between channel terraces. Hence for the longer slope will have a greater total soil loss just because it is bigger. Steeper terrain slopes cause higher runoff velocities, more splash downhill and faster flow. Both of these factors contribute to soil erosion.

The effect of slope steepness on soil erosion [43] is defined as follows:

- Considerable erosion occurs even when the soil surface is level, but the increase with slope steepness over a broad range of steepness is relatively small; and
- Erosion only doubled for a steepness change from 2-20% and the erosion rate tends to level of. A slight increase in detachment rate probably occurs as the raindrops strike at a greater and greater angle, but this effect should not cause a major change in total splash detachment.

In order to estimate the impact of slope length and slope steepness on the assessment of soil erosion risk in Mediterranean areas in general and in the study area in particular, the following categories will be considered [45].

- 0-5% : areas with very low erosion risk;
- 5-15% : areas with moderate erosion risk;
- 15-30% : areas with high erosion risk; and
- >30% : areas with extremely high erosion risk.

In this research work the map shows the erosion risk categories were developed from slope percentage map (created from DEM); and according this map values of 0-15% refers areas with very low to moderate erosion risk; 15-30% refers areas with high erosion risk; and >30% refers to areas with extremely high erosion risk. The map of erosion risk for study area is presented in Figure 5.9. Similarly the number of grid cells (NPix) and their respective areas under each erosion risk categories (topographic classes) are given in Table 5.3.

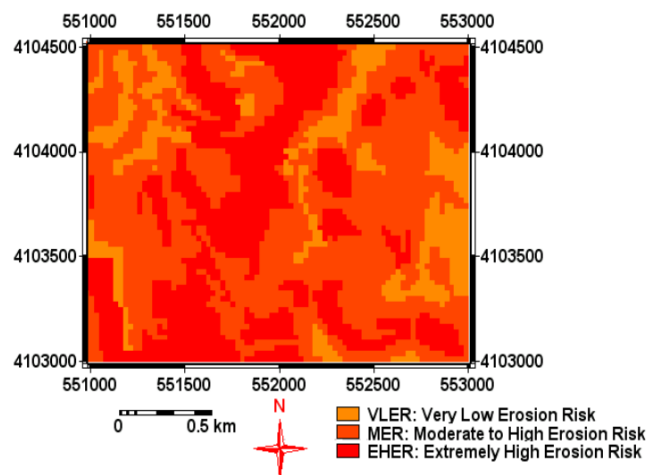


Figure 5.9: Map of erosion risk categories.

1

Slope Factor (LS) Values

¹SLOPEPCT: slope percentage; NPix: pixel number

<i>SLOPEPCT</i>	<i>NPix</i>	<i>Area (ha)</i>	<i>Definition</i>
0-5%	64	41.4	areas with very low erosion risk
5-15%	363	90.8	areas with moderate erosion risk
15-30%	748	84.3	areas with high erosion risk
greater than 30%	1169	83.6	areas with extremely high erosion risk

Table 5.3: The number of grid cells (NPix) and their respective areas calculated from Topographic factor (LS) interface by ILWIS RUSLE 3.0 and their erosion risk categories

In computation of slope factors (LS) from DEM (pixel size of 25 m) using the ILWIS 3.0 RUSLE Topographic Factor (LS) interface the following equations were considered.

- $L_RUSLE = ((PIXSIZE(slopedeg)*3.280833)/72.6)^{m_RUSLE}$;
- $m_RUSLE = \beta_RUSLE / (1 + \beta_RUSLE)$;
- $\beta_RUSLE = ((\sin(slopedeg*3.14/180)/0.0896)) / (3 * (\sin(slopedeg*3.14/180)^{0.8} + 0.56))$;
- $S_RUSLE = FF((PIXSIZE(slopedeg) > 4.572009) \text{ and } (slope < 9), (10.8 * \sin(slopedeg*3.14/180)) + 0.03, ?)$; and
- $LS = L_RUSLE * S_RUSLE$

Where,

- L, slope length factor;
- m-RUSLE, slope length exponent.
The slope length exponent m is related to the rill to interrill ratio, β of rill erosion (caused by flow) to interrill erosion (principally caused by raindrop impact); and
- S, slope steepness factor (S).

Since ILWIS 3.0 RUSLE Topographic factor (LS) interface calculates the L factor, S factor and LS factor for each grid cells (pixels) and has 2344 values for these grid cells, their values (LS) not given under this subsection; but their values (LS) including other factors or variables values that were used to compute soil loss (A) are given in RUSLE LS table under soil loss (A) subsection.

The map shows values of LS factor is presented in Figure 5.10

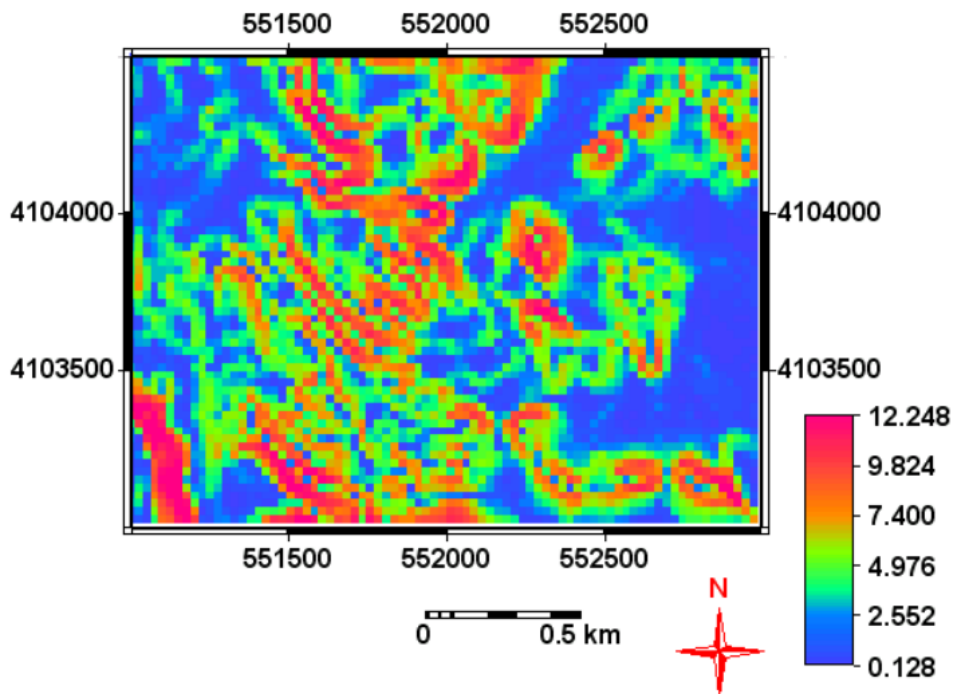


Figure 5.10: Map of LS factor with value ranges from 0.128-12.248.

5.3.4 COVER-MANAGEMENT FACTOR (C)

C is the cover-management factor. The C-factor is used to reflect the effect of cropping and management practices on erosion rates. Cover management factor is the factor used most often to compare the relative impacts of management options on conservation plans. The C-factor indicates how the conservation plan will affect the average annual soil loss and how that soil-loss potential will be distributed in time during construction activities, crop rotations or other management schemes.

Main effects of cover management are:

Rainfall interception; and

Reduce velocity of runoff.

Interception: reduces raindrop impact, maintains infiltration, reduces sealing and crusting etc.

Kinetic energy absorbed and dissipated by plant cover rather than by the soil.

The study area (northwest of Tabernas) with 300 ha or 3 square kilo meter is located in semi-arid climatic zone, and the areas suitable for agricultural activity are highly located in areas of sediment deposition or where the erosion risk is very low, and that the study of soil erosion by water was not considered in agricultural areas. It has to be clear that, in this research work there present that areas of sediment deposition when classifying physiographic zones, but as that of the sediment deposition area size is too small and covered by consolidated conglomerates, the areas classified as sediment deposition does not represent the areas of agriculture. Furthermore estimation of soil erosion by water in agricultural area requires the following input data and as there were no such input data at hand to estimate cover and management factor (C) this research was considered soil loss on natural soil erosion. The input data that use as input to estimate cover and management factor (C) or Soil loss Ratio (SLR) in agricultural area are: Prior land use (PLU), canopy cover (CC), surface roughness (SR), surface cover (SC) and soil moisture (SM); and which each variables also requires many sub-variables

5.3. PREDICTION OF SOIL EROSION BY WATER USING RUSLE

as input to estimate soil loss ratio (SLR). Therefore, due to the above mentioned reasons the estimation of soil erosion by water was implemented in areas of non-agriculture or where soil erosion is very high.

The estimation of cover factor (C) was based on the NDVI classified values and the classified NDVI includes the major classes such as water, bare soils (bareland) and vegetation. The table derived from NDVI classified is presented in Figure 5.11.


	npix	npixpct	Area
-0.41	4891	0.05	1498.3
0.03	6351820	64.86	1945834.1
1.0	3436241	35.09	1052667.6
Min	4891	0.05	1498.3
Max	6351820	64.86	1945834.1
Avg	3264317	33.33	1000000.0
Std	3176955	32.44	973237.3
Sum	9792952	100.00	3000000.0

Figure 5.11: Table of land cover classes.

As the NDVI classified indicates the percentage of vegetation is 35% and that of bare soils (bareland) is 65% and this bare soil percentage represents the cover factor (C).

5.3.5 CONSERVATION PRACTICE FACTOR (P)

P is the conservation practice factor. The RUSLE P-factor reflects the impact of support practices in the average annual erosion rate. It is the ratio of soil loss with contouring and/or strip cropping to that with straight row farming up-and-down slope. As with the other factors, the P-factor differentiates between cropland and rangeland or permanent pasture. As the study of this research work to estimate soil erosion using RUSLE modelling was applied in the area of non-agriculture or on natural (geological) erosion, it was considered that there was no conservation practice (P) in non-agricultural areas. Therefore as the conservation practice factor (P) value ranges from 0.0-1.0 and the highest value is assigned to areas with no conservation practice, the maximum value for P that is 1.0 is assigned to this research work area.

5.3.6 SOIL LOSS (A)

$$A = R * K * C * LS * P$$

The estimated annual soil loss values for year 1984 is based on the values of monthly rainfall data, Landsat TM 7203 (1984) imagery, slope factors (LS) and soil data from different sources. In estimation of annual soil loss (A) Soil erodibility factor (K) values was taken from soil with organic matter (Wischeier soil-erodibility

nomograph equation) and soil without organic matter (the mean geometric particle size (world soil data set)) to compare and contrast the effect of organic matter on soil erosion by water. Depending upon different values of slope factors (LS), the computation of annual soil loss value was computed by inserting all variables in RUSLE LS table, and the annual soil loss values computed for each grid cells in the RUSLE LS table. And after the annual soil loss (A) values computed for each grid cells for entire study area the total sum of annual soil loss (A) values was used to analyze and discuss the final result.

According to computed annual soil loss (A) values of different soil erodibility factors (K), the annual soil loss value has 16727.95 ton/300ha (55.76 ton/ha) for soil with organic matter; and 44607.94 ton/300ha (148.70 ton/ha) for soil without organic matter.

The summarized annual soil loss values and different input variables (factors) are presented in Table 5.12 and 5.13; but as the table contains 2344 rows and 17 columns, part of rows and the important variables from columns are given in the table. Similarly due to reasons defined above part but all of the continuation of this table is given in the appendix. Annual soil loss (A) maps of study area for soil samples with and without organic matter are presented in Figure 5.14 and 5.15.²

SLOPE	PC Area (m ²)	L_RUSLE	S_RUSLE	LS_RUSLE	R	P	K1	C	A1 (ton/grid cells)
0	5000	1	0.03	0.03	121.88	1	0.015	0.65	0.04
0.4	13125	1.009	0.073	0.074	121.88	1	0.015	0.65	0.09
0.57	3750	1.011	0.09	0.091	121.88	1	0.015	0.65	0.11
0.8	8125	1.015	0.117	0.119	121.88	1	0.015	0.65	0.14
0.89	8125	1.017	0.126	0.128	121.88	1	0.015	0.65	0.15
1.13	3750	1.02	0.153	0.156	121.88	1	0.015	0.65	0.18
1.26	2500	1.022	0.166	0.169	121.88	1	0.015	0.65	0.2
1.44	6250	1.024	0.186	0.191	121.88	1	0.015	0.65	0.23
1.6	6875	1.026	0.203	0.209	121.88	1	0.015	0.65	0.25
1.65	8125	1.026	0.207	0.213	121.88	1	0.015	0.65	0.25
1.7	1250	1.027	0.213	0.218	121.88	1	0.015	0.65	0.26
1.79	3125	1.028	0.222	0.228	121.88	1	0.015	0.65	0.27
2	12500	1.03	0.247	0.254	121.88	1	0.015	0.65	0.3
2.04	12500	1.031	0.25	0.258	121.88	1	0.015	0.65	0.31
...
Total	3000000								16727.95

Figure 5.12: Table of annual soil loss (A) for soil with organic matter and dots indicate that the continuation of values for each grid cells.

²K1: soil erosivity factor for soil with organic matter; A1: soil loss for soil with organic matter; K2: soil loss for soil without organic matter; A2: soil loss for soil without organic matter

5.3. PREDICTION OF SOIL EROSION BY WATER USING RUSLE

SLOPEPCT	Area (m ²)	L_RUSLE	S_RUSLE	LS_RUSL/R	P	K2	C	A2 (ton/grid cells)
0	5000	1	0.03	0.03	121.88	1	0.04	0.095
0.4	13125	1.009	0.073	0.074	121.88	1	0.04	0.234
0.57	3750	1.011	0.09	0.091	121.88	1	0.04	0.289
0.8	8125	1.015	0.117	0.119	121.88	1	0.04	0.376
0.89	8125	1.017	0.126	0.128	121.88	1	0.04	0.406
1.13	3750	1.02	0.153	0.156	121.88	1	0.04	0.493
1.26	2500	1.022	0.166	0.169	121.88	1	0.04	0.536
1.44	6250	1.024	0.186	0.191	121.88	1	0.04	0.605
1.6	6875	1.026	0.203	0.209	121.88	1	0.04	0.661
1.65	8125	1.026	0.207	0.213	121.88	1	0.04	0.674
1.7	1250	1.027	0.213	0.218	121.88	1	0.04	0.692
1.79	3125	1.028	0.222	0.228	121.88	1	0.04	0.724
2	12500	1.03	0.247	0.254	121.88	1	0.04	0.805
2.04	12500	1.031	0.25	0.258	121.88	1	0.04	0.818
...
Total	3000000							44607.944

Figure 5.13: Table of annual soil loss (A) for soil without organic matter and dots indicate that the continuation of values for each grid cells.

5.4 CONCLUSIONS

To estimate rainfall erosivity factor (R) or $(EI30)_{min}$ intensity per 30 minutes and hourly precipitation (mm) are the data that use as an input. So, during this thesis work as there was no intensity and hourly precipitation data, the only solution to estimate erosivity factor (R) was considered and the equation that uses the monthly and annual precipitation (mm) input to estimate annual erosivity factor was applied.

Slope factors LS depends generally on the slope steepness than on the slope length and similarly the soil erosion risk also depends on the slope percentage. Depending on slope percentage areas 0-5% erosion risk and 15-30% high erosion risk, and >30% extremely high erosion risk were classified. In the study area from total of 300.00ha (3 square kilo meter) about 41.38 ha or 14% has the slope% of 0-5; 90.8 ha or 30% has the slope % of 5-15; 84.25 ha or 28% has the slope % of 15-30, and 83.56 ha or 28% has the slope % of above 30. In addition to geologic factors and thickness of soil horizons that not grater than 25 cm, and which makes the area vulnerable to soil erosion, this value of slope % might have helped to estimate the soil erosion risk in the study area.

The estimation of land cover was computed grounding on Landsat TM imagery (NDVI) acquired on single date in single month, and as a result comparison of soil erosion from month to month with in a year was not computed and only annual soil loss was computed. Not only but also it was good that to estimate soil loss (erosion) by water for year 2002, but the absence of datasets such as Landsat TM imagery and rainfall (precipitation) for year 2002 forced the estimation of soil loss on available datasets of year 1984.

The computed annual *Soil loss* values show that, for soils samples with organic matter (Wischmeier soil nomograph) soil loss (A1) has a value of 16727.95 ton/300ha or(55.8 ton/ha); and for soils without organic matter and computed in the mean geometric particle size (world soil data set) soil loss (A2) value is 44607.94 ton/300ha or (148.7 ton/ha). These values tell that organic matter reduces soil erodibility, because it reduces the susceptibility of the soil to detachment, and it increases infiltration, which reduces runoff.

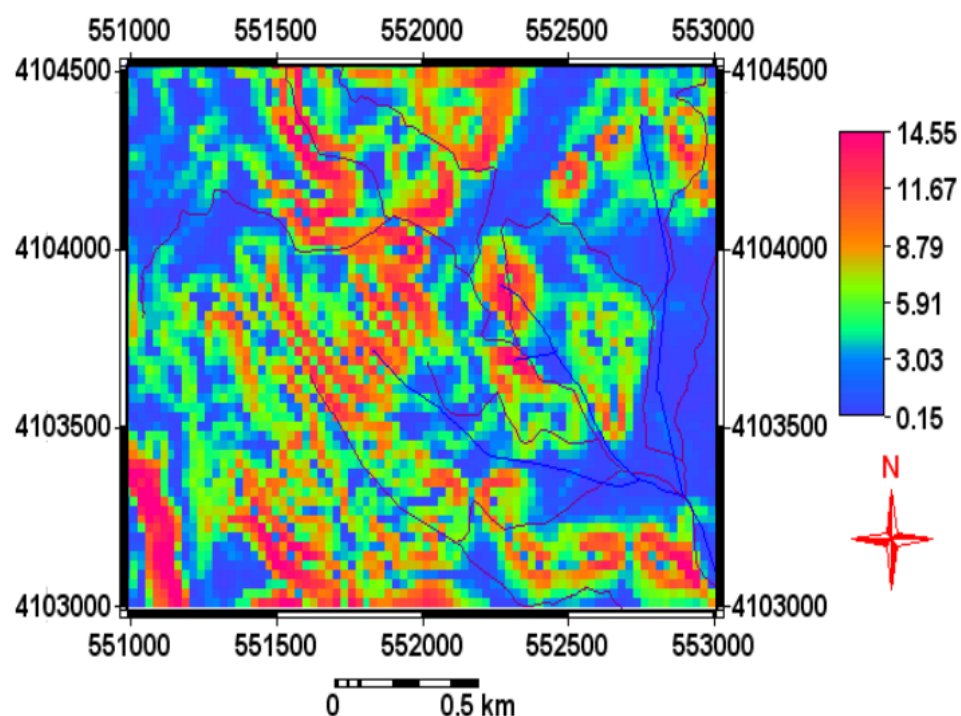


Figure 5.14: Map of annual soil loss (A1) for soil sample with organic matter and values vary for each grid cells ranging from 0.15-14.55 ton/grid cells.

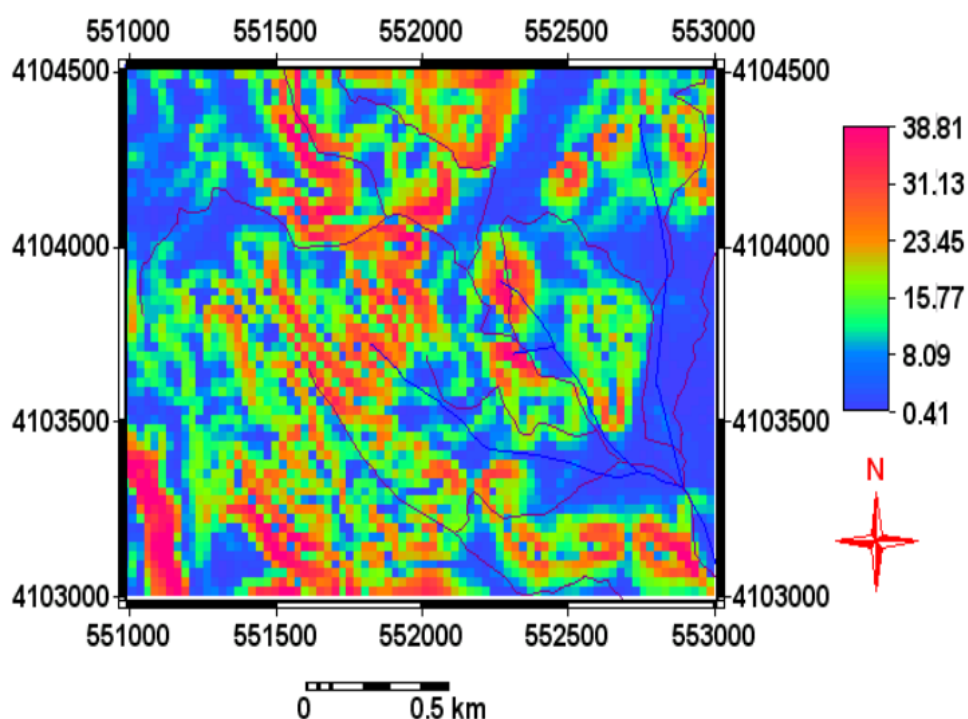


Figure 5.15: Map of annual soil loss (A2) for soil sample without organic matter and values vary for each grid cells ranging from 0.41-38.81 ton/grid cells.

Chapter 6

RESULTS ANALYSIS AND DISCUSSION

6.1 INTRODUCTION

The objective of this chapter is to evaluate the results obtained in the study of soil erosion or soil loss. The influences of natural environmental conditions and their implications on soil erosion will also be discussed. The evaluation of the spatial distribution through time of the different processes will be used to infer tentatively erodibility of the soil. All information obtained through this work will permit to have a first approach to explain the natural causes that contribute to the soil erosion process in the research area (northwest of Tabernas).

6.2 RAINFALL-RUNOFF EROSION FACTOR (K)

According to the estimated erosion factor (R) shown in chapter five the estimation of R is highly based on monthly rainfall depths (mm) and annual rainfall (mm), and when the monthly rainfall is high the annual rainfall is high, and also annual rainfall erosion factor (R) is high. On the other hand as there was no rainfall data for specific rainy days with single storm and rainfall intensity for 30 minutes or one hour, the kinetic energy of rainfall storm was not computed to estimate the effect of kinetic energy of rainfall in the area. But depending on the annual rainfall erosion factor (R) the following erosion dynamics were concluded. There are five annual rainfall erosion factor (R) classes [15] such as; very low, low, medium, high and very high. A relatively low annual rainfall erosion factor (R) can contain high individual storm erosion. In semi-arid countries there is a relatively low annual rainfall erosion factor (R), because of less vegetation, bare soil, and therefore possibly relative high erosion dynamics (problems). Countries with medium rainfall erosion factor (R) can have little erosion problems due to e.g. evenly distributed seasonal rainfall erosion factor (R), good vegetation cover and low reliefs. According to the annual rainfall erosion factor (R) classification, Tabernas in general and the study area (northwest of Tabernas) in particular with annual rainfall erosion factor (R) 121.88 (MJ*mm/ha*hr); 7.16 (100.ft.ton-ft*inch/acre*hr) and 12.19 (KJ*mm/m²*hr) falls under very low annual rainfall erosion factor (R) and has high erosion problems. Table of classification of annual rainfall erosion factor (R) in different units, and graph of monthly rainfall amounts and associated sum square of monthly rainfall per annual rainfall are presented in Figure 6.1 and 6.2.

	R(US_units)	R(SI_units)	R(SI_units) _{ss}
Legend-class(*)	-1	-2	-3
Very low	<30	<500	<50
low	30-60	500-1000	50-100
medium	60-180	1000-3000	100-300
high	180-350	3000-6000	300-600
Very high	>350(**)	>6000(**)	>600

(1) $R(\text{US customary units}) = 100 \cdot \text{ft} \cdot \text{ton} \cdot f \cdot \text{inch} / \text{acre} \cdot \text{hr}$

(2) $R(\text{SI customary units}) = \text{MJ} \cdot \text{mm} / \text{ha} \cdot \text{hr}$ ♦ Recommended R unit.

(3) $R(\text{SI}) \text{ Sensu stricto} = \text{KJ} \cdot \text{mm} / \text{m}^2 \cdot \text{hr}$.

(*): Example of a 5 class legend: user-defined and/or locally adaptable.

(**): Extremes up to >500 (US) or $\pm 10,000$ R(SI) possible.

Note: class boundaries between US and SI systems not exactly equivalent but rounded-off.

Figure 6.1: Table of typical annual erosivity range classification in different unit systems [15]

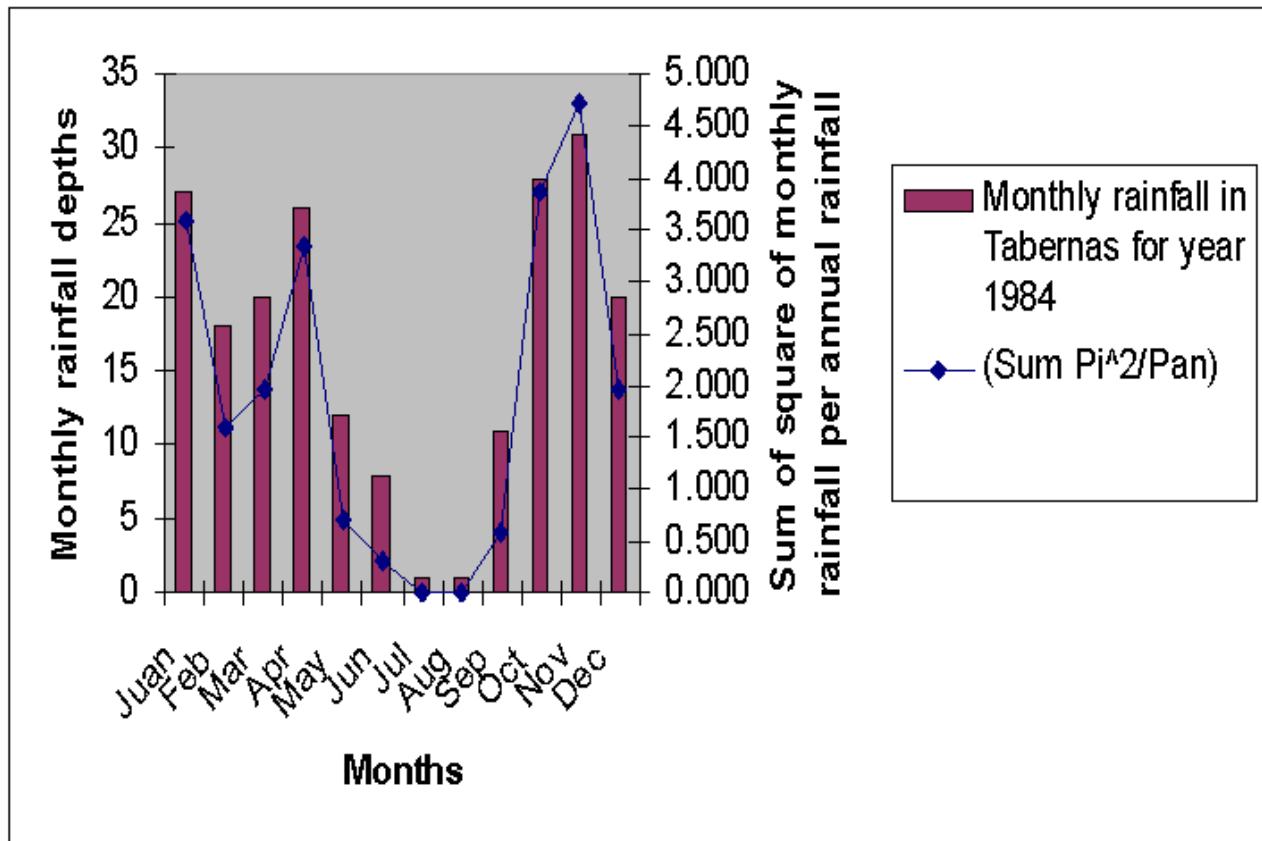


Figure 6.2: Graph of monthly rainfall amounts and associated sum of square of monthly rainfall per annual rainfall

6.3 SOIL ERODIBILITY FACTOR (K)

The estimated soil erodibility factor (K) values show that the erodibility of soil is dependent on soils particle diameter and soils with high concentration of clay are least susceptible to soil erosion, while soils with high silt concentration are highly susceptible for soil erosion than that of soils rich in clay and sand size particles (texture). Similarly the soils with organic matter are least susceptible to soil erosion than soils without organic matter. Graph of soil erodibility factor (K) and particle diameter with moving average trendline is presented in Figure 6.3.

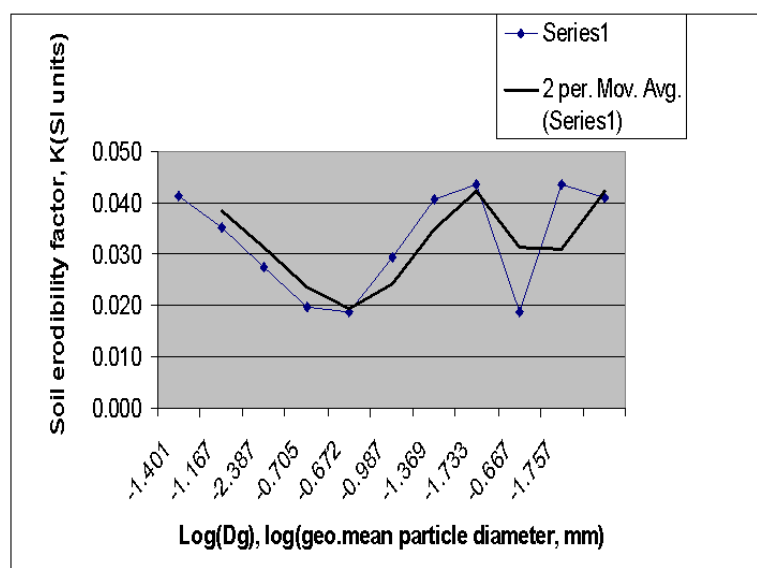


Figure 6.3: Graph of soil erodibility as a function of mean geometric particle diameter (Dg) in S.I. units or (ton/ha per MJ/ha*mm/hr)

6.4 SLOPE LENGTH AND SLOPE STEEPNESS FACTOR (LS)

It was mentioned in chapter five that the topography of the study area is rugged with non-uniform terrains and slope degree value ranges from 0-51.18; slope percentage value ranges from 0-124.28; L.RUSLE value ranges from 1.00-1.095; S.RUSLE values ranges from 0.03-13.585 and L.RUSLE value ranges from 0.03-14.872. Depending on values of slope factors (LS) for each grid cells that differ from grid to grid, the estimated soil loss values also differs from one grid cells to another grid cells.

6.5 COVER-MANAGEMENT FACTOR (C)

As the area of study (northwest of Tabernas) is located in the semi-arid zone of the Mediterranean region and the land cover of the area is highly dominated by *desert grasses, bush and shrubs*; most of the areas are bare soils (bareland) and as a result the value for management factor(C) is high. In this research work according to the value obtained from NDVI, the value of C factor is 0.65 (65%).

6.6 SENSITIVITY ANALYSIS

The extent of that predictions of soil loss by the model are affected by small changes in the values of the input parameters was assessed using partial differentiation. The results of estimated values show that soil loss predictions are most sensitive to changes in slope steepness or S.RUSLE with *polynomial trendline (relation)* and less sensitive to slope length or L.RUSLE with *logarithmic trendline (relation)*. Similarly soil erosion by water is highly sensitive to spatial change of slopes and as a result the difference in values of soil loss ranges from 0.1 ton/grid cells for slope% of 0; and 47.13 ton/grid cells for slope% of 124.28. Also soil loss is sensitive to soil particles diameter and that it was observed

by varying the values of soil erodibility factor (K)(by varying the percent of particles size) from 10% upto 100% while other factors remain constant, and the same is true for rainfall erosivity factor (R) (approved by varying monthly rainfall or precipitation (mm) from % 10 upto % 100 while the other variables remain constant) and cover-management factor ((C) (by decreasing the percentage of land cover)). As there was no conservation practice (P factor) in the study area, sensitivity analysis was not computed for this variable. It should be clear that the sensitivity analysis for slope factors (LS) was done by using regression operation as that of other variables, but as the slope factors (LS) have no single value for study areas as that of other variables, the table of sensitivity analysis for this variable is not presented together with the graph as the others.

According to the results of sensitivity analysis, soil loss is highly sensitive to slope factors (LS) and equally but less sensitive to rainfall erosivity factor (R), soil erodibility factor (K) and cover management factor (C). As it can be seen in the following graphs all factor but LS factor have linear trendline (relation) versus soil loss (A).

In conclusion, as there was no previously carried out research works regarding estimation of soil loss by water in the study area that uses as references to validate the estimated soil loss value, the result of this research work of estimation of soil loss by water was not validated.

The graphs show the computed sensitivity analysis for each factor vs soil loss (A) are presented in Figure 6.4 6.6 and 6.7.

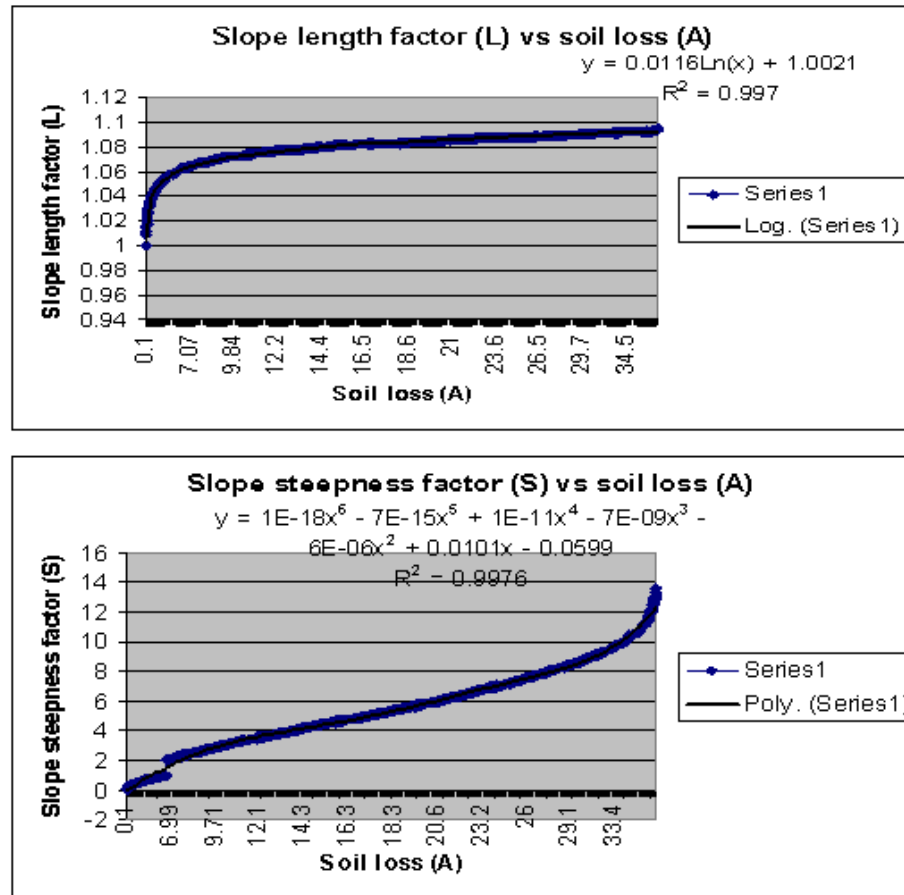


Figure 6.4: Graph of Slope length factor (L) and Slope steepness factor (S) vs Soil loss (A)

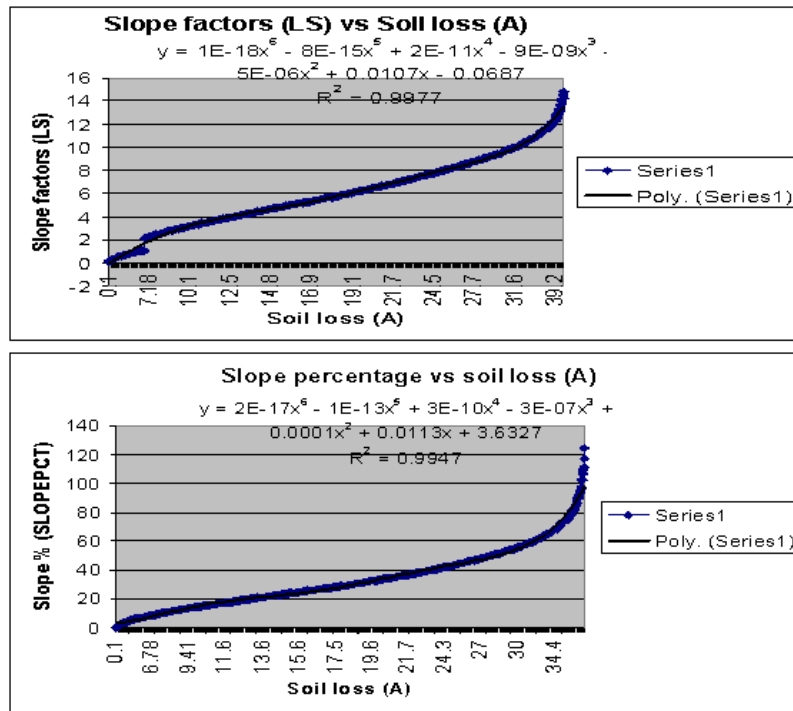


Figure 6.5: Graphs of Slope factors (LS) and Slope % (SLOPEPCT) vs soil loss (A)

LS factor (max	C factor	K factor	P factor	Increase (%)	R factor	Soil loss (A)
14	0.65	0.015	1	0	121.88	17.673
14	0.65	0.015	1	10	134.068	19.440
14	0.65	0.015	1	20	146.256	21.207
14	0.65	0.015	1	30	158.444	22.975
14	0.65	0.015	1	40	170.632	24.742
14	0.65	0.015	1	50	182.82	26.509
14	0.65	0.015	1	60	195.008	28.277
14	0.65	0.015	1	70	207.196	30.044
14	0.65	0.015	1	80	219.384	31.811
14	0.65	0.015	1	90	231.572	33.578
14	0.65	0.015	1	100	243.76	35.346

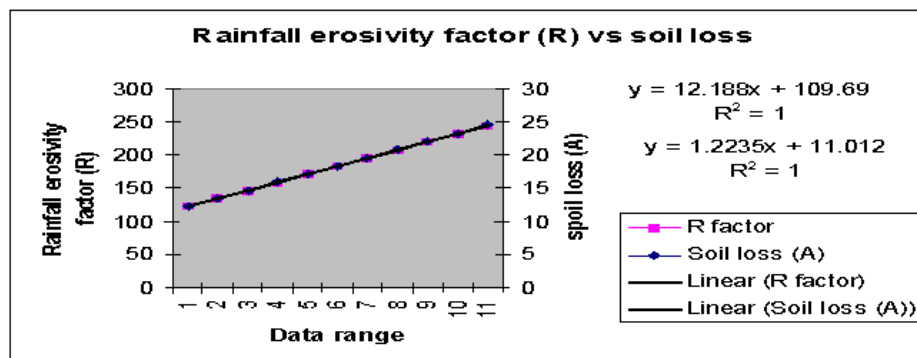


Figure 6.6: Graph of Rainfall erosivity factor(R) vs Soil loss (A)

6.6. SENSITIVITY ANALYSIS

LS factor (max C factor	R factor ®	P factor	Increase (%)	K factor	Soil loss (A)	
14	0.65	121.88	1	0	0.015	17.673
14	0.65	121.88	1	10	0.0165	19.440
14	0.65	121.88	1	20	0.018	21.207
14	0.65	121.88	1	30	0.0195	22.975
14	0.65	121.88	1	40	0.021	24.742
14	0.65	121.88	1	50	0.0225	26.509
14	0.65	121.88	1	60	0.024	28.277
14	0.65	121.88	1	70	0.0255	30.044
14	0.65	121.88	1	80	0.027	31.811
14	0.65	121.88	1	90	0.0285	33.578
14	0.65	121.88	1	100	0.03	35.346

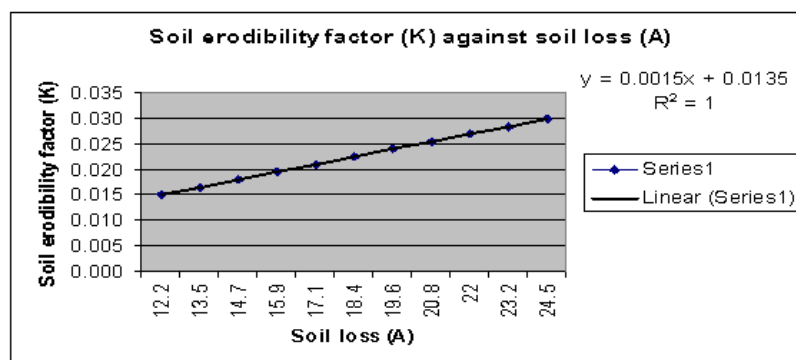


Figure 6.7: Graph of Soil erodibility factor (K) vs soil loss (A)

LS factor (max K factor	R factor ®	P factor	Increase (%)	C factor	Soil loss (A)	
14	0.015	121.88	1	0	0.65	17.673
14	0.015	121.88	1	10	0.715	19.440
14	0.015	121.88	1	20	0.78	21.207
14	0.015	121.88	1	30	0.845	22.975
14	0.015	121.88	1	40	0.91	24.742
14	0.015	121.88	1	50	0.975	26.509
14	0.015	121.88	1	60	1.04	28.277
14	0.015	121.88	1	70	1.105	30.044
14	0.015	121.88	1	80	1.17	31.811
14	0.015	121.88	1	90	1.235	33.578
14	0.015	121.88	1	100	1.3	35.346

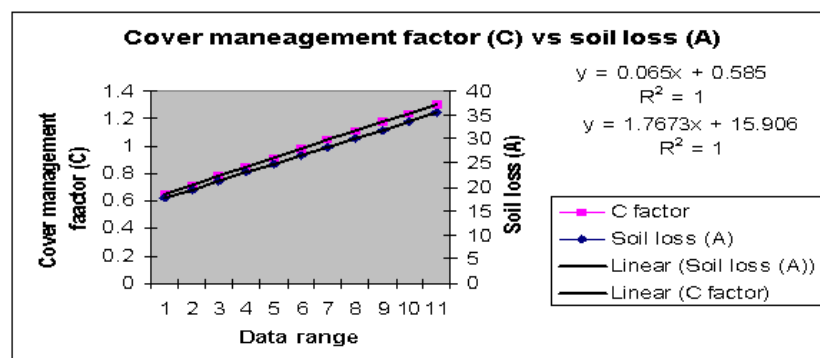


Figure 6.8: Graph of Cover management factor (C) vs Soil loss (A)

Chapter 7

CONCLUSIONS AND RECOMMENDATIONS

7.1 CONCLUSIONS

In study area, northwest of Tabernas, the soil erosion by water was serious due to the following reasons:

- Decrease of tree biomass due to the lack of regeneration;
- Engineering constructions (roads);
- Rugged topography;
- Sparse vegetation cover;
- Thin soil horizon; and
- Tectonic (land slides) activities.

From this it follows that the effects of soil erosion will result in the following environmental problems:

- Less vegetation cover;
- Loss of soil productivity when needed for agricultural activities;
- Contamination of ground water and additional expenses to control soil erosion and water treatment; and
- Random changes in the micro-topography of the slope surfaces.
- For such thin stony and loose soils, soil erosion by water is the crucial problem and even very modest rates of erosion exceed geological rates of soil development through weathering, so that soils gradually become more stonier.
- Provided that the soil of the study areas is highly consists of stones and as the non-stony fraction declines by erosion, they begin to a reduction in effective water storage capacity. Beyond this limit, increases in erosion lead to progressive loss of water storage and further enhance the erosion rates and facilitates the arid dry conditions.
- The Normalized Difference vegetation index (NDVI) is a measure of the amount of green cover at the earth surface and the quantification of NDVI is relative and not absolute. Furthermore the information acquired from NDVI does not fully but partly substitute the information acquired from fieldwork.
- ILWIS 3.0 RUSLE Topographic Factor (LS) interface is useful software to calculate Slope Degrees; Slope Percentage; Pixel numbers; Area; Beta.RUSLE; m.RUSLE; L.RUSLE; S.RUSLE and LS.RUSLE per grid cells.

- Soil loss by water is most sensitive to changes in slope steepness or S.RUSLE and less sensitive to slope length or L.RUSLE. Soil loss is highly sensitive to slope factors (LS) and equally but less sensitive to rainfall erosivity factor (R), soil erodibility factor (K) and cover management factor (C).

7.2 RECOMMENDATIONS

- Once erosion starts on previously sustainable land, the erosion processes develop as follows: the advanced interrill erosion develops the rill erosion and the advanced rill erosion develops gully erosion. Hence once gullies developed they are almost impossible to eradicate or manage, leading to the abandonment of the land as *badlands* while the infrastructures like inter valley and hills road cut, and high power electric transmission tower installation are also imposing their impact on the environment.
- So in order to control the intensity of natural erosion or soil loss by water to certain limit, the conservation erosion controlling trends has to be followed.
- Similarly conservation practice like deep rooted desert trees and trees with broad canopy that intercept rainfall have to be planted, and in addition to that another conservation practices like complete stripping or terracing of the soil to a bedrock slope has to be practised. Because terraces reduce the slope length and sometimes the slope steepness. Those conservation practices and cover management may minimize the effect of soil erosion (soil loss) by rainfall-runoff, but other environmental problems that facilitate soil erosion like landslide and mass movement are unmanageable.
- During infrastructure development such as access road construction or expansion, proper environmental considerations are recommended.
- Field data is recommended as ground truth to confirm the accuracy of the information acquired from new technology or remote sensing (RS); in this research case classified NDVI from Landsat TM imagery for major cover classes (water, bare soils and vegetation).
- Finally, further investigation is recommended to dig out the extent of soil erosion (soil loss) problems and mitigate those problems that prevailing in the area.

References

- [1] C.Pieri; J.dumanski; A.Hamblin and A.Young. Land quality indicators. Technical report, World Bank, 1995.
- [2] S.; L. Lonergan; J.P. Platt; E. Platzman Allerton and E.McClelland. Palaeomagnetic rotations in the eastern betic cordillera, southern spain. Technical report 119: 225-241, Earth planet sci. Lett., 1993.
- [3] Taye Almayehu. Environmental indicator mapping and change detection using remotely sensed data and indicator based approach. Msc thesis, ITC, Enschede, February 2001.
- [4] L.Recatala; J.C.Colomer; B.Cornelis; and A.G. Fabbri. Integrated environmental mapping for applying indicators of environmental quality at a multi-hierarchical level in mediterranean areas affected by desertification. Technical report, ITC, ECOSUD, 2001.
- [5] Brown, 1987.
- [6] H.J. Buiten and J.G.P.W. Clevers. *Land Observation by Remote Sensing*, volume 3. Gordon and Breach Science Publisher, Amsterdam, 1993.
- [7] A. Cendrero and D.W. Fischer. A procedure for assessing the environmental quality of coastal areas for planning and management. Journal, 1997.
- [8] Banks; C.J. and Warburton. Mid-crustal detachment in the betic system of southern spain. Technical report 191: 275-289, 1991.
- [9] A.J. Conacher and m. Sala. Land degradation in mediterranean environments of the word: nature and extent, causes and solutions. Technical report, 1998.
- [10] R.U. Cooke and J.C. Doornkamp. *Geomorphology in Environmental Management*. Clarendon Press, Oxford, second edition, 1990. A New Introduction.
- [11] A. D.Abrahams and A.J.Parsons. Geomorphology of desert environments. Chapman and Hall, 1994.
- [12] Ministerio de Agricultura Pesca Y Alimentacion;ICONA and Consejo Superior de Investigaciones Cientificas. Proyecto lucdeme, mapa de suelos escala 1:10,000. map, 1987.
- [13] Plataforma Solar de Almeria. Plataforma solar de almeria. Annual technical report, Tabernas, Spain, 1999.
- [14] E. Puga Diaz de Federico, A.; M.T. Gomez Pugnaire and F.P. Sassi. *New problems in the Sierra Nevada Complex (Betic Cordilleras, Spain)*, volume 10. Neues Jahrb. Geol. Paleontol. Montash., 1979.
- [15] C.Manaerts dr.ir. *Modelling water erosion, sedimentation and chemical transport*. Environmental Watershed hydrology Water resources Division ITC, April 2002.
- [16] C.g. Egeler and O.J. Simon. Orogenic evolution of the betic zone (betic cordilleras, spain) with emphasis on the nappe structures. Technical report 48: 296-305, Geol. Mijnbouw, 1969.
- [17] ELANEM. identifying and assessing quantitative indicator and indices to measure environmental quality. First annual report, scientific report, ELANEM, Ensenada, Mexico, February 2000.

- [18] FAO. Guías para la descripción de perfiles de suelos. Technical report, FAO, 1977.
- [19] FAO. Desertification, drought and their consequences. Website, May 1996.
- [20] Dr Hazel Faulkner. Gully erosion studies in Spain, 26 November 2002.
- [21] W; Hilgen F.J. Fortuin, A.R; Krijgsman and F.J. Sierro. Late Miocene Mediterranean desiccation: topography and significance of the 'salinity crisis' erosion surface on-land in southeast Spain. Technical report 133, 167-174, 2000.
- [22] V.; J.M.M. Martínez; M. Orozco García-Dueñas and J.I. Soto. Plis-nappes, cisaillements syna post-metamorphiques et cisaillements ductiles-fragiles en distension dans les Nevado-Filabrides (cordillères bétiques, Espagne), C. R. Acad. Technical Report 11, 307, 1389-1395, Espagne, 1988.
- [23] M.; A.C. López-Garrido; P. Rivas; C. Sanz de Galdeano García-Hernández and J.A. Vera. Mesozoic paleogeographic evolution of the external zones of the Betic Cordillera. Technical report 59: 155-168, Geol. Mijnbouw, 1980.
- [24] Geiger. Technical report.
- [25] G. Govers. *Spatial and temporal variation in rill development processes at the Huldenberg experimental site*. Number pp 31-32. CATENA suppl 8, 1987.
- [26] Rodríguez Puebla. Technical report, 1998.
- [27] L.R. Oldeman; R.T.A. Hakkeling and W.G. Sombroek. World map of human-induced soil degradation, an explanatory note. Technical report, UNEP and ISRIC, 1990.
- [28] A.R. Harrison and P. Garg. *Multi-spectral Classification for Vegetation Monitoring in Semi-arid Landscapes Susceptible to Soil Erosion and Desertification*. Gordon and Breach Science Publisher, 1991.
- [29] A. D. Howard. *Geology in Environmental Planning*. McGraw-Hill Book Company, New York, 1978.
- [30] N. Hudson. *Soil Conservation*. 320. Ithaca, Cornell University Press, New York, 1971.
- [31] N.W. Hudson. Soil conservation. Technical report, Basford, 1985.
- [32] P. W. J. M. Huibregtse, M. van Alebeek, E. A. Zaal, and C. Biermann. *Strike-slip tectonics and the Evolution of Neogene intramontane basins in the Internal Betic Cordilleras of SE Spain*. Free University of Amsterdam, Amsterdam, 1998.
- [33] Zinck J.A. *Physiography and soils. Soil survey courses subject matter*. 156. ITC, K6, Enschede, The Netherlands, 1988.
- [34] J.C. O'Connor. Environmental performance monitoring indicators. Technical Report 3, 1994.
- [35] Friends of the Oldman v. Canada et al Justice La Forest. Defining impact assessment. website, 1991.
- [36] Tilahun Chernet Kerse. Mapping salinity using multispectral and hyperspectral data in Tabernas, south east Spain. MSc thesis, ITC, Enschede, February 2002.
- [37] K. Kleverlaan. *Gordo megabed: A possible seismic in a Tortonian submarine fan, Tabernas Basin, Province Almería, SE Spain-Sed*. Geology 51: 165-180. 1987.
- [38] K. Kleverlaan. Neogene history of the Tabernas basin (SE Spain) and its Tortonian submarine fan development. Free University, Department of Earth Sciences, p. Oox 7161, 1007 MC Amsterdam, The Netherlands, 26 April 1989.
- [39] Dante E. Margate. The use of hyperspectral data in identifying desert like soil features in Tabernas, southeast Spain. Master's thesis, ITC, Enschede, February 2000.
- [40] K.G. Renard; G.R. Foster; G.A. Weesies; D.K. McCool and D.C. Yoder. *Predicting Soil Loss by Water. A guide to Conservation planning with the revised universal Soil loss Equation (RUSLE)*. Number Agricultural Handbook number 703, 404pp. United States Department of Agriculture (USDA), Washington, DC 20250, January 1997.

-
- [41] MEDALUS. River basin modelling for decision support in land management. Web site, 1993.
- [42] J. Hill; S. Sommer; W. Mehl and J. Megier. A conceptual framework for mapping and monitoring the degradation of mediterranean ecosystems with remote sensing. Experts workshop on the use of remote sensing for land degradation and desertification monitoring in the mediterranean basin, State of the art and future research 16732 EN, EUR, 1994.
- [43] Foster G.R. Meyer, L.D. and m.J.M. Romkens. Source of soil eroded by water from up land slopes, in present and prospective technology for predicting sediment yields and sources. Technical report, U.S. Department of Agriculture Sedimentation Laboratory, U.S. Oxford, 1975.
- [44] R.P. Morgan. soil erosion. Technical report, Longman, 1979.
- [45] R.P.C Morgan. *Agriculture; Erosion assessment and modelling*. Number 354. Brussels, European Commission, 1988.
- [46] E. Partheniades. Erosion and deposition of cohesive soils. journals of the Hydraulics Division of the American Society of Civil Engineers, v. 91, no. HY1, p. 105-139, 1965.
- [47] Juan Fernando Palacio Pemberty. Assessment of morphodynamic processes and soil pollution as indicators of land degradation. a case study in the tabernas area, southeastern spain. Msc thesis, ITC, March 2002.
- [48] G. Pickup and V. Chewings. Identifying and measuring land degradation processes using remote sensing. Experts workshop on the use of remote sensing for land degradation and desertification monitoring in the mediterranean basin, State of the art and future research 16732 EN, EUR, 1994.
- [49] J.P; B.van den Eeckhout; E.Janzen; G.Konert; O.J.simon Platt and R.weiijermars. The structure and tectonic evolution of the aguillon fold-nappe, sierra alhamilla, betic cordilleras, se spain-j. 1983.
- [50] L. Recatala, A. G. Fabbri, J. A. Zinck, E. Frances, and J. Sanchez. *Environmental indicators for Assessing and Monitoring Desertification and its influence on Environmental Quality in Mediterranean Arid Environments*. Number 12. ITC and CIDE, Enschede, 2000.
- [51] C Roquero de Laburu. Causas y efectos de la erosion en el medio natural de almeria. Proceedings on the seminar on arid zones, Almeria, 1982.
- [52] Riley patrick Arulanandan Kandiah Sargunam, Arunachalan and R.B. Krone. physio-chemical factors in erosion of cohesive soils. Journals of Hydraulics Division of the American Society of Civil Engineers, v. 99,no. HY3, p. 555-558, 1973.
- [53] SCOPE. Technical report.
- [54] A. Sole-Benet and A. Calvo. Influence of micro-relief patterns and plant cover on runoff related processes in badlands from tabernas SE Spain. Technical report 31:33-38, CATENA, 1997.
- [55] A. Strahler. *The Earth Sciences*. Harper and Row, New York, second edition, 1971.
- [56] C. W. Thornthwaite. *An approach to ward a rational classification of climate*, volume 38. Unpublished, 1948.
- [57] UNEP. Status of desertification and implementation of the united nations plan of action to combat desertification. web site, 1991.
- [58] UNEP. A new response to an age-old problems. web site, 2000.
- [59] UNESCO. World distribution of arid regions. Website, 1977.
- [60] F. van der Meer. Fieldwork and excursion guide to the geology of the tabernas-sorbas basin. ITC, 2000.
- [61] A. S. Walker. *Deserts: Geology and Resources*. Unpublished, 2000.

- [62] A.B.; J.P. Platt Watts and P. Buhl. Tectonic evolution of the alboran sea basin, basin res. Technical report 5: 153-177, 1993.
- [63] R. Weijermars. *Geology and tectonics of the Betic Zone, SE Spain*, volume 31. Elsevier Science publishers B. V., Amsterdam, 1991.

WEBSITES

<http://www.pasture.ecn.purdue.edu/engelb/abe526/wshddelin/wshddelin.html>

<http://www.citimac.unican.es/elanem.html>

<http://www.grid2.cr.usgs.gov/des/unced.php3.html>

<http://www.fao.org/waicent/faoinfo/sustdev/EPdirect/EPan0005.htm>

<http://www.gdrc.org/uem/eia/define.html>

<http://www.science.plym.ac.uk/DEPARTMENTS/GEOLOGY/AcadStaff.html>

<http://www.ncl.ac.uk/wrgi/wrsrl/projects/medalus/medalus.html>

<http://www.asp.wlv.ac.uk/Level7.asp.html>

<http://www.topsoil.nserl.purdue.edu/nserlweb/weppmain/overview/intro.html>

<http://www.un.org/ecosocdev/geninfo/sustdev/desert.htm>

<http://www.un.org/ecosocdev/geninfo/sustdev/desert.htm>

<http://www.un.org/ecosocdev/geninfo/sustdev/desert.htm>

<http://www.un.org/ecosocdev/geninfo/sustdev/desert.htm>

<http://www.bsyse.wsu.edu/saxton/soilwater/soilwater.htm>

http://www.LERGHomepage_files/hazel.htm

http://www.iwr.msu.edu/ouyangda/rusle/r_factor.htm

Chapter 8

APPENDICES

APPENDIX



Degraded land in Tabernas area



**Bad land geomorphology in Tabernas area. Department
of Geography, King's College London (1996)**

Figure 8.1: Map of degraded and bad land geomorphology in Tabernas area

ALMERIA AEROP.												
Periodo: 1968-1990 Altitud (m): 21 Latitud: 36 50 35 Longitud: 2 23 17												
MES	T	TM	Tm	R	H	DR	DN	DT	DF	DH	DD	I
ENE	12.5	16.8	8.1	27	70	6.2	0.0	0.2	0.8	0.0	7.5	186
FEB	13.0	17.5	8.5	18	68	5.0	0.0	0.3	1.1	0.0	5.3	187
MAR	14.6	18.9	9.8	20	66	4.9	0.0	0.2	1.2	0.0	5.6	213
ABR	16.1	20.7	11.6	26	65	5.9	0.0	0.8	0.4	0.0	4.7	235
MAY	18.8	23.3	14.2	12	67	4.1	0.0	0.7	0.6	0.0	6.1	300
JUN	22.3	27.0	17.7	8	65	2.0	0.0	0.7	0.5	0.0	10.9	323
JUL	25.4	30.1	20.8	1	64	1.0	0.0	0.5	0.6	0.0	18.4	343
AGO	26.0	30.4	21.6	1	66	1.3	0.0	0.6	0.4	0.0	14.6	311
SEP	24.1	28.5	19.6	11	66	2.5	0.0	0.6	0.2	0.0	10.0	254
OCT	19.9	24.4	15.7	28	69	4.7	0.0	1.0	0.5	0.0	5.6	220
NOV	16.2	20.5	11.9	31	70	6.0	0.0	0.7	0.5	0.0	5.7	185
DIC	13.3	17.7	9.0	20	69	5.8	0.0	0.4	0.9	0.0	6.6	181
AÑO	18.5	23.0	14.0	204	67	49.4	0.0	6.7	7.7	0.0	101.0	2937

LEYENDA

- T Temperatura media mensual/anual (°C)
- TM Media mensual/anual de las temperaturas máximas diarias (°C)
- Tm Media mensual/anual de las temperaturas mínimas diarias (°C)
- R Precipitación mensual/anual media (mm)
- H Humedad relativa media (%)
- DR Número medio mensual/anual de días de precipitación superior o igual a 1 mm
- DN Número medio mensual/anual de días de nieve
- DT Número medio mensual/anual de días de tormenta
- DF Número medio mensual/anual de días de niebla
- DH Número medio mensual/anual de días de helada
- DD Número medio mensual/anual de días despejados
- I Número medio mensual/anual de horas de sol

Figure 8.2: Table of Rainfall and Temperature data for Almeria area from Spanish Meteorological Office (1968-1990).

	Method 1					
Fraction n.	Size range	fi(%)	mi(mm)	ln(mi)	fi.ln(mi)	sum
Clay	0-0.0002	25.56	0.001	-6.90776	-176.528	
silt	0.002-0.05	22.85	0.026	-3.64966	-83.3947	
vf.sand	0.05-0.1		0.076	-2.57702	0	
f.sand	0.1-0.2		0.175	-1.74297	0	
m.sand	0.2-0.5		0.375	-0.98083	0	
l.sand	0.5-2.0		0.75	-0.28768	0	
Total sand	0.05-2.0	51.60	0.5	-0.69315	-35.7629	
Fine earth	fraction tot	100.00			-295.685	sum
Total sand	0.05-2.0					
Calculation using mean geom.particle diam.equation						
			Values			
geom.mean part.diam.DG			0.051982			
		Log(Dg)	-1.28415			
$K = (0.0034 + 0.0405 \cdot \exp(-0.5 \cdot ((\log(Dg) + 1.66)/0.71)^2))$						
Soil erodibility (K(SI-1)			0.031	ton/ha per MJ/ha*mm/h		
K-values K(SI-2)			0.031	kg/m^2 per KJ/m^2*mm/h		
	K(pfs,US)		0.238	ton/acre per 100-ft.ton/acre*inch		
	K(EU,sp)		2.377	ton/ha per 100.J/m^2*cm/h		

Figure 8.3: Example of equation of mean geometric particle diameter(word data set)

Station no.	Sample no	Lab. code	Clay %	Silt%	Sand%	EC (ds/m)	PH
25	6	T1	19.75	44.14	36.11	4.63	8.6
27	8	T2	31.36	1.56	67.08	0.51	8.7
40	13	T3	58.79	38.86	2.35	0.42	8.8
46	14	T4	5.49	19.91	74.60	5.22	8.8
7	4	T5	9.75	8.40	81.85	0.14	9
115	43	T6	2.69	47.76	49.55	2.37	7.9
76	28	T7	4.07	74.64	21.29	2.55	8
114	42	T8	32.00	44.24	23.77	2.25	8
63	21	T9	6.85	14.07	79.08	4.68	8.6
69	25	T10	22.94	65.17	11.89	11.76	8.8
98	38	T11	*	*	*	0.83	8.8
58	19	T12	37.73	47.66	14.61	2.74	9
Range			5.49-58.79	1.56-74.64	2.35-81.85	0.14-11.76	7.9-9
Median			19.75	47.66	36.11	-	-

Particle size measurements for the 12 selected

Figure 8.4: Table of soil texture data (Tilahun, 2002)

Sample NO	Ca con.	Na con.	Mg con	SAR	pH	EC	UTM_X	UTM_Y
T 1	41.19	7.43	6.8	1.072539854	8.5	0.38	547644	4094364
T 2	132.15	231.8	34.6	17.95066369	8.1	2.53	547480	4094648
T 3	93.23	18.37	15.72	1.759930586	8.4	0.77	549628	4096552
T 4	35.22	1.35	3.28	0.2175722	9	0.14	552728	4107648
T 5	25.74	2.8	4.15	0.51214752	9	0.11	553410	4102966
T 6	453.54	291.67	28.28	13.28762762	8.6	4.63	552705	4104040
T 7	352.48	13.46	11.17	0.705835121	8	1.98	552876	4103799
T 8	44.67	36.64	5.83	5.155962808	8.7	0.51	553216	4103417
T 9	-0.06	-0.27	0.5	-0.407040315	8.9	0.11	544032	4104343
T 10	25.71	3.16	3.5	0.584684127	8.7	0.18	547152	4100839
T 11	399.10	737.05	69.81	34.03716313	8.9	3.69	547352	4100839
T 12	436.76	66.09	53.54	2.984728313	8.2	2.47	547650	4100688
T 13	24.88	1.65	3.39	0.310328055	8.8	0.42	547501	4099920
T 14	528.22	449.72	27.27	19.08118395	8.8	5.22	552419	4101976
T 15	510.43	203.29	19.55	8.830283127	8.6	3.77	552985	4102800
T 16	108.00	582.00	61.18	44.7454082	8.7	9.23	552562	4102534
T 17	489.43	282.89	51.98	12.15787745	8.6	4.28	550882	4100169
T 18	20.77	5.28	5.47	1.030746828	8.5	0.17	558601	4109624
T 19	198.07	139.92	13.4	9.621779805	9	2.74	549133	4097095

Table shows the coordinate system and sample number for soil sample data

Figure 8.5: Table of coordinate system and sample number for soil texture data (Tilahun, 2002)

Area (m^2)	L_RUSLE	S_RUSLE	LS_RUSLE	P	C	K1	A1 (ton/grids)	K2	A2 (ton/grids)	
10625	1.032	0.262	0.27	121.88	1	0.65	0.015	0.32	0.04	0.856
625	1.033	0.275	0.284	121.88	1	0.65	0.015	0.34	0.04	0.9
7500	1.033	0.282	0.292	121.88	1	0.65	0.015	0.35	0.04	0.925
8125	1.034	0.288	0.298	121.88	1	0.65	0.015	0.35	0.04	0.944
10625	1.034	0.292	0.302	121.88	1	0.65	0.015	0.36	0.04	0.957
10000	1.035	0.303	0.314	121.88	1	0.65	0.015	0.37	0.04	0.994
5000	1.035	0.307	0.318	121.88	1	0.65	0.015	0.38	0.04	1.007
7500	1.036	0.32	0.332	121.88	1	0.65	0.015	0.39	0.04	1.051
2500	1.037	0.331	0.344	121.88	1	0.65	0.015	0.41	0.04	1.089
11250	1.037	0.335	0.348	121.88	1	0.65	0.015	0.41	0.04	1.102
7500	1.038	0.341	0.354	121.88	1	0.65	0.015	0.42	0.04	1.121
9375	1.038	0.345	0.358	121.88	1	0.65	0.015	0.43	0.04	1.134
3750	1.039	0.358	0.372	121.88	1	0.65	0.015	0.44	0.04	1.178
15625	1.04	0.367	0.382	121.88	1	0.65	0.015	0.45	0.04	1.21
...	

Figure 8.6: Table of ILWIS 3.0 RUSLE Topographic Factor (LS) interface for soil loss estimated per grid cells that continued from chapter 5 and; K1 and A1 indicates values for soil with organic matter while K2 and A2 indicates values for soil without organic matter

SLOPEPCT	Area (m ²)	L_RUSLE	S_RUSLE	LS_RUSLE	R	P	C	K1	A1 (ton/grids)	K2	A2 (ton/grids)
3.2	3125	1.04	0.375	0.39	121.88	1	0.65	0.015	0.46	0.04	1.235
3.22	11250	1.04	0.379	0.394	121.88	1	0.65	0.015	0.47	0.04	1.248
3.3	3750	1.041	0.386	0.402	121.88	1	0.65	0.015	0.48	0.04	1.273
3.39	4375	1.041	0.395	0.412	121.88	1	0.65	0.015	0.49	0.04	1.305
3.42	3750	1.042	0.399	0.416	121.88	1	0.65	0.015	0.49	0.04	1.318
3.44	7500	1.042	0.401	0.418	121.88	1	0.65	0.015	0.5	0.04	1.324
3.58	1250	1.043	0.416	0.434	121.88	1	0.65	0.015	0.52	0.04	1.375
3.6	6250	1.043	0.418	0.436	121.88	1	0.65	0.015	0.52	0.04	1.381
3.62	3750	1.043	0.42	0.438	121.88	1	0.65	0.015	0.52	0.04	1.388
3.69	5000	1.043	0.427	0.446	121.88	1	0.65	0.015	0.53	0.04	1.413
3.69	6250	1.043	0.427	0.446	121.88	1	0.65	0.015	0.53	0.04	1.413
3.77	1875	1.044	0.437	0.456	121.88	1	0.65	0.015	0.54	0.04	1.445
3.79	3750	1.044	0.439	0.458	121.88	1	0.65	0.015	0.54	0.04	1.451
3.94	5625	1.045	0.456	0.476	121.88	1	0.65	0.015	0.57	0.04	1.509
...

Figure 8.7: Table of ILWIS 3.0 RUSLE Topographic Factor (LS) interface for soil loss estimated per grid cells continued.

SLOPEPCT	Area (m ²)	L_RUSLE	S_RUSLE	LS_RUSLE	R	P	C	K1	A1 (ton/grids)	K2	A2 (ton/grids)
3.96	3125	1.045	0.458	0.478	121.88	1	0.65	0.015	0.57	0.04	1.515
4	11250	1.045	0.461	0.482	121.88	1	0.65	0.015	0.57	0.04	1.528
4.02	3750	1.045	0.463	0.484	121.88	1	0.65	0.015	0.58	0.04	1.534
4.08	4375	1.046	0.471	0.492	121.88	1	0.65	0.015	0.58	0.04	1.56
4.12	3750	1.046	0.475	0.496	121.88	1	0.65	0.015	0.59	0.04	1.572
4.18	7500	1.046	0.48	0.502	121.88	1	0.65	0.015	0.6	0.04	1.591
4.25	1250	1.046	0.488	0.51	121.88	1	0.65	0.015	0.61	0.04	1.617
4.31	6250	1.047	0.495	0.518	121.88	1	0.65	0.015	0.62	0.04	1.643
4.33	3750	1.047	0.497	0.52	121.88	1	0.65	0.015	0.62	0.04	1.649
4.4	5000	1.047	0.505	0.528	121.88	1	0.65	0.015	0.63	0.04	1.675
4.42	6250	1.047	0.507	0.53	121.88	1	0.65	0.015	0.63	0.04	1.681
4.47	1875	1.048	0.512	0.536	121.88	1	0.65	0.015	0.64	0.04	1.7
4.53	3750	1.048	0.518	0.543	121.88	1	0.65	0.015	0.64	0.04	1.719
4.56	5625	1.048	0.522	0.547	121.88	1	0.65	0.015	0.65	0.04	1.732
...

Figure 8.8: Table of ILWIS 3.0 RUSLE Topographic Factor (LS) interface for soil loss estimated per grid cells continued.

SLOPEPCT	Area (m^2)	L_RUSLE	S_RUSLE	LS_RUSLE	R	P	C	K1	A1 (ton/grids)	K2	A2 (ton/grids)
4.66	11250	1.049	0.533	0.559	12.88	1	0.65	0.015	0.66	0.04	1.515
4.68	3125	1.049	0.535	0.561	12.88	1	0.65	0.015	0.67	0.04	1.528
4.8	2500	1.049	0.548	0.575	12.88	1	0.65	0.015	0.68	0.04	1.534
4.82	7500	1.049	0.55	0.577	12.88	1	0.65	0.015	0.69	0.04	1.56
4.83	6250	1.049	0.552	0.579	12.88	1	0.65	0.015	0.69	0.04	1.572
4.87	13125	1.05	0.555	0.583	12.88	1	0.65	0.015	0.69	0.04	1.591
4.88	2500	1.05	0.557	0.585	12.88	1	0.65	0.015	0.7	0.04	1.617
4.95	4375	1.05	0.563	0.591	12.88	1	0.65	0.015	0.7	0.04	1.643
5.01	5625	1.05	0.571	0.599	12.88	1	0.65	0.015	0.71	0.04	1.649
5.06	3125	1.05	0.576	0.605	12.88	1	0.65	0.015	0.72	0.04	1.675
5.09	1250	1.05	0.578	0.607	12.88	1	0.65	0.015	0.72	0.04	1.681
5.12	2500	1.051	0.582	0.611	12.88	1	0.65	0.015	0.73	0.04	1.7
5.2	1875	1.051	0.591	0.621	12.88	1	0.65	0.015	0.74	0.04	1.719
5.22	3750	1.051	0.593	0.623	12.88	1	0.65	0.015	0.74	0.04	1.732
...

Figure 8.9: Table of ILWIS 3.0 RUSLE Topographic Factor (LS) interface for soil loss estimated per grid cells continued.

SLOPEPCT	Area (m^2)	L_RUSLE	S_RUSLE	LS_RUSLE	R	P	C	K1	A1 (ton/grids)	K2	A2 (ton/grids)
5.26	3750	1.051	0.597	0.627	121.88	1	0.65	0.015	0.75	0.04	1.988
5.34	1250	1.052	0.604	0.635	121.88	1	0.65	0.015	0.76	0.04	2.014
5.37	5000	1.052	0.608	0.64	121.88	1	0.65	0.015	0.76	0.04	2.027
5.38	3750	1.052	0.61	0.642	121.88	1	0.65	0.015	0.76	0.04	2.033
5.44	3125	1.052	0.616	0.648	121.88	1	0.65	0.015	0.77	0.04	2.052
5.56	6250	1.053	0.629	0.662	121.88	1	0.65	0.015	0.79	0.04	2.097
5.57	2500	1.053	0.631	0.664	121.88	1	0.65	0.015	0.79	0.04	2.104
5.6	1875	1.053	0.634	0.668	121.88	1	0.65	0.015	0.79	0.04	2.116
5.61	4375	1.053	0.634	0.668	121.88	1	0.65	0.015	0.79	0.04	2.116
5.66	6875	1.053	0.64	0.674	121.88	1	0.65	0.015	0.8	0.04	2.136
5.69	4375	1.053	0.642	0.676	121.88	1	0.65	0.015	0.8	0.04	2.142
5.73	3125	1.053	0.648	0.682	121.88	1	0.65	0.015	0.81	0.04	2.161
5.77	2500	1.053	0.651	0.686	121.88	1	0.65	0.015	0.82	0.04	2.174
5.82	1875	1.054	0.657	0.692	121.88	1	0.65	0.015	0.82	0.04	2.193
...

Figure 8.10: Table of ILWIS 3.0 RUSLE Topographic Factor (LS) interface for soil loss estimated per grid cells continued.